NOT TO BE CITED WITHOUT PRIOR
REFERENCE TO THE AUTHOR(S)

Northwest Atlantic Fisheries Organization

Serial No. N6559 **NAFO SCR Doc. 16/018**

SCIENTIFIC COUNCIL MEETING – JUNE 2016

Environmental Conditions in the Labrador Sea during 2015

I. Yashayaev, E.J.H. Head, K. Azetsu-Scott, E. Devred, M. Ringuette, Z. Wang, and S. Punshon

Department of Fisheries and Oceans, Maritimes Region
Ocean and Ecosystem Sciences Division, Bedford Institute of Oceanography
P.O. Box 1006, Dartmouth, N.S. B2Y 4A2

Abstract

The Dec-Jan-Feb (DJF) composite North Atlantic Oscillation (NAO) index was strongly positive in 2015, the highest one on record. During the winter convection season, the NCEP reanalysis of surface air temperature indicated below normal temperature conditions with a negative anomaly ranging between 0 – 4°C in the Labrador Sea. Sea surface temperature anomalies (SST) estimated using AVHRR remote-sensed data in the central Labrador Sea were also below normal temperature, with negative seasonal anomalies ranging between 0.438 and 1.188 ˚C The Labrador Shelf ice extent was slightly above normal in the months of January and March (reference period: 1981-2010); however, in the northern part of the Labrador Sea, the total sea ice extent was slightly below normal in winter. Wintertime convection in 2015 reached 1850 m, which is even deeper than the 1600 m seen in 2014. DIC and pH are following their usual inverted pattern yielding a sustained decline rate in pH of 0.003 units per year since 1996. Silicate concentration in the newly ventilated layer is also decreasing, following the same trend as has been observed in the rest of the Northwest Atlantic. Intense phytoplankton production in spring over the entire Labrador Basin led to one of the highest levels of seasonal primary production observed since 1995. The apparent lower abundance of *Calanus finmarchicus* and other organisms in the mesozooplankton followed trends observed elsewhere, but may have been exacerbated, because of net clogging at most stations in the central Labrador Sea.

Introduction

Since 1990, the Ocean and Ecosystem Sciences Division at the Bedford Institute of Oceanography has carried out annual occupations of a hydrographic section across the Labrador Sea (Figure 1) The section was designated as AR7W (Atlantic Repeat Hydrography Line 7 West) in the World Ocean Circulation Experiment (WOCE). Other than traditional physical seawater characteristics (temperature, salinity, density, currents), these surveys also include chemical (e.g., dissolved oxygen, nutrients, chlorofluorocarbons, sulfur hexafluoride, total inorganic carbon, pH) and biological measurements (e.g., bacteria until 2012, phytoplankton and mesozooplankton). The AR7W line is the major component of the Canadian Department of Fisheries and Oceans (DFO) Atlantic Zone Off-shelf Monitoring Program (AZOMP) and the main Canadian contribution to the international Global Climate Observing System (GCOS) and to the (international) Climate Variability (CLIVAR) component of the World Climate Research Programme (WCRP). The section spans approximately 880 km from the 130 m contour on the inshore Labrador shelf to the 125 m contour on the West Greenland shelf. Sea ice sometimes limits coverage at the ends of the section. DFO also contributes to the international Argo program by deploying floats in the Labrador Sea and managing and processing the Argo data streams. The importance of international Labrador Sea monitoring and AZOMP, in particular was discussed and emphasized in the recent special issue of Progress in Oceanography (Yashayaev et al., 2015;

Kieke and Yashayaev et al., 2015). Indeed, the Labrador Sea can viewed as receiving and blending basin, heart and lung of the Atlantic Ocean and Earth's climate (Yashayaev et al., 2015), and the annual AZOMP multidisciplinary survey of the Labrador Sea (primarily AR7W and profiling Argo floats) present invaluable contribution to the ongoing international ocean and climate monitoring and research effort.

Since this transect has been surveyed for more than two decades, the data now exist to make a meaningful examination of multiyear trends. In addition, the near real-time temperature and salinity of the Argo float armada that became available in 2002 draw a large-scale picture of the hydrographic structure and circulation of the Labrador Sea. The variation of the hydrographic variables (temperature, salinity, density, dissolved oxygen, etc.) show seasonal, inter-annual, decadal and longer-term variability, largely governed by the changing contributions of several factors including; 1) winter heat losses to the atmosphere, heat and salt gained from Atlantic Waters carried northward into the Labrador Sea by the West Greenland Current, 2) freshwater input from ice and melt from the Arctic and Greenland, continental runoff and precipitation. Occasional severe winters lead to strong cooling of the upper layers, and the resulting increases in the surface density cause the water column to mix to great depths. By the end of winter, convective mixing may penetrate deeper than 1500 m and in extreme cases deeper than 2000 m. Milder winters lead to lesser heat losses, thus stronger influence of heat and salt passed from the warm and saline Atlantic Waters, and stronger stratification in the subsurface (>200 m) layers. The atmospheric conditions, largely under the influence of the North Atlantic Oscillation (NAO) index play an important role in the establishment of deep convection events in the Labrador Sea, which can help explain the development of significant long-term hydrographic phenomena in the region. Under global warming scenarios, the increasing freshwater inputs from the melting Greenland glacier and the Arctic Ocean also contribute to the hydrographic variations at seasonal, inter-annual and longer time scales. Continuation of the annual oceanographic sampling on the AR7W line and the on-going support of the Argo float array will help to improve and deepen our understanding of the multi-scale processes and variability, providing a more comprehensive understanding of the role of the Labrador Sea in global climate system as well as of the dominant physical processes in the regional ecosystem.

A sequence of severe winters in the early 1990s led to deep convection that was most intense in 1993–1994. Milder atmospheric conditions prevailed in the following years and the upper layers gradually regained their vertical stratification in density and other physical and chemical properties. The trends of increasing temperature and decreasing density established in the upper 1000 m of the Labrador Sea with the cessation of extreme convection of the first half of the 1990's were interrupted in the winters of 2000, 2002 and 2008, 2012, 2014 and 2015 when observations showed that deep convection in the central Labrador Sea often approached and even exceeded 1500 m.

Atmospheric System

North Atlantic Oscillation

The NAO is an important teleconnection pattern influencing atmospheric processes in the Labrador Sea (Barnston and Livezey, 1987; Hausser et al., 2015). When the North Atlantic Oscillation (NAO) is in its positive phase, low-pressure anomalies over the Icelandic region and throughout the Arctic combined with high-pressure anomalies across the subtropical Atlantic produce stronger-than-average westerlies across the mid-latitudes. Conditions over the northwestern Atlantic including the Labrador Sea region are colder and drier than average. A negative NAO indicates weakening of both the Icelandic low and Azores high, which decreases the pressure gradient across the North Atlantic resulting in weakening of the westerlies and brings warmer conditions than usual. Both NAO phases are associated with basin-wide changes in the intensity and location of the North Atlantic jet stream and storm track, and in large-scale modulations of the zonal and meridional heat and moisture transport (Hurrell, 1995), resulting in the modification of the temperature and precipitation patterns.

The NAO exhibits considerable interseasonal to interdecadal variability, and prolonged periods of both positive and negative phases seem to have more influence on convection in the Labrador Sea than short-term fluctuations (Yashayaev, 2007). The wintertime NAO also exhibits significant multi-decadal variability (Hurrell, 1995). An upward trend of the NAO index from the 1960s through the 1990s was noted by Visbeck et al (2001), although since the peak in the 1990s there has been a slight downward trend. Recent studies reveal an atmospheric circulation pattern, complementary to NAO, which becomes more prominent in years of low NAO (Hausser et al., 2015). Further study of this phenomenon will help to improve understanding and forecasting capabilities of atmospheric and oceanic conditions.

In 2010, the NAO index reached a record low (Figure 2), leading to warmer than normal conditions, confirmed by Argo float data and the AR7W survey. In 2011, the NAO index rebounded from the record low but still remained well below the 30-year average (1981-2010). In 2012, however, the NAO index was strongly positive (12 mbar), up to a level comparable to those in early 1990s showing the highest winter index over the last twenty years. There was a significant change in the winter NAO index in 2013, when it became moderately negative (-3 mbar). In 2014, the NAO index returned to its high positive phase, slightly lower than the 2012 value, making it the second highest in the last twenty years, leading to colder than normal winter conditions in the region. In 2015 there was another high NAO event, when it was in fact the highest value on record.

Surface Air Temperature

The NCEP/NCAR Reanalysis Project is a joint project between the National Centers for Environmental Prediction (NCEP) and the National Center for Atmospheric Research (NCAR). The goal of this joint effort is to produce new atmospheric analyses using historical data (1948 onwards) to produce analyses of the current atmospheric state (Kalnay et al., 1996).

The NCEP reanalysis of surface air temperature indicates below normal conditions with an anomaly ranging between 0 and 4°C in the Labrador Sea during winter, the biggest winter negative anomalies being in the northern part of Baffin Bay (>4°C). Most of Labrador Sea was ~1°C below normal during the spring, with the strongest negative anomaly in the northern region of the Labrador Sea. In summer the Eastern Labrador Sea and Baffin Bay were approximately 1°C above normal, while in the western part of the Labrador Sea was cooler by 1°C. Fall brought a negative anomaly of 1 – 4°Cover the entire Labrador Sea and Baffin Bay (Figure 3).

Sea Surface Conditions

Sea Surface Temperature

We use AVHRR remote-sensed estimation to capture the SST variations over the full year cycle in the Labrador Sea (Figure 4). The dataset only covers the southern part of the Labrador Sea but it is divided so we can separate the Labrador shelf/slope from the Central basin and the Greenland shelf/slope. All 3 regions were colder than normal with negative yearly average anomalies in the Labrador Shelf/slope, the Central basin and the Greenland shelf/slope respectively of 0.344, 0.682 and 0.588°C. Only the winter SST on the Labrador Shelf had a positive anomaly; all other region/seasons had negative average anomalies ranging from -0.25to -1.125 ^{o}C. We did not use the larger spatial scale dataset from NCEP/NCAR reanalysis, because it generates in inconsistencies in SST field.

Sea Ice

The sea ice data are obtained from The U.S. National Snow and Ice Data Center. Ice concentration in the coastal zone of Labrador Shelf was slightly above normal in the winter months of 2015 (5%; reference period: 1979-2000), while the ice edge region presented below normal concentration, indicating a possible reduction in ice extent in these areas (Figure 5). In the northern part of the Labrador Sea, sea ice concentration showed a similar trend during the winter time, then became significantly above normal in the eastern sector. The sea ice extents did not show clear changes compared with the 1970-2000 climatology except for a significant increase in March in the eastern part of the northern Labrador Sea, consistent with the increased ice concentration in this area.

To give a quantitative and clearer view of the ice extent changes in the Davis Strait (63-68^{o}N), the northern Labrador Sea (58-63 ^{o}N), and the Labrador Shelf (53-58 ^{o}N), the ice extents for the three regions were estimated by summing the areas with ice concentration higher than 85%. Figure 6 shows the time series of monthly ice extent anomalies from 1979 to 2015, with the monthly mean climatology based on the data from 1981 to 2010 (Note, however that the climatology used in Figure 5 was for the 1979 to 2000 period). The wintertime ice extent in Davis Strait was slightly above normal (10,000 km^2), which is consistent with the 4^{o}C below average wintertime air temperature in this region. The northern Labrador Sea ice extent was below normal in wintertime as a whole (20,000 km^2). On the Labrador Shelf, the ice extent was close to the long term mean for wintertime, although January and March did have slightly above normal ice cover.

AR7W Hydrography

Drifting sea ice generally prevents access to the Labrador Shelf before mid-May; notwithstanding this constraint, the annual AR7W surveys normally take place as early in the spring as practical to provide a consistent view of interannual changes resulting from the large seasonal changes in physical, chemical, and biological properties. In addition to the AR7W Line, a full AZOMP survey also includes sampling of the extended Halifax Line (XHL) to monitor variability on the Scotian Rise and Slope in the deep western boundary flows of the North Atlantic and to obtain additional information on oceanographic and lower-trophic-level variability of the Slope Water affecting the Scotian and adjacent shelves (http://www.bio.gc.ca/science/monitoring-monitorage/azomp-pmzao/azomp-pmzao-eng.php). The survey in 2015 was conducted aboard the *CCGS Hudson* from the 2nd to the 26rd of May (See Figure 1).

Change in temperature and salinity in the upper layers of the Labrador Sea occur in response to changes in: atmospheric forcing, warm and saline inflows via the Irminger Current and shallower fresh and cold inflows via the West Greenland and Labrador Currents, together with and freshwater inputs originating from precipitation, runoff and glacier melt. Seasonal cycles in each of these three forcing terms drive a strong seasonal cycle in the properties of the upper layers of the Labrador Sea. Significant decadal variability has also been observed in the central Labrador Sea. While there has been relatively little variability below 2500 m, there have been significant decade-long events in the upper 2000 m. A period of warming and increasing salinity during the mid-1960s to mid-1970s was followed by a reverse period of cooling and freshening during the 1990s, characterised by deep winter convection that filled the upper two kilometers of the Labrador Sea of the water column with cold and fresh water: in some years convection reached 2400 m and possibly deeper. Milder winters in recent years have produced more limited amounts of mode waters, which have gradually become warmer, saltier, and less dense than they were a decade and a half ago. This recent trend changed abruptly during the cold winter of 2008 when deep convection to 1600 m was observed. The environmental conditions that contributed to the 2008 deep convection have been documented by Yashayaev and Loder (2009).

The advent of the International Argo Progam has provided the oceanographic community with unprecedented, year-round observations of temperature and salinity in the Labrador Sea. A composite of data from Argo floats in the Labrador Sea is presented in Figure 7. The time series clearly demonstrates the seasonal and interannual variability over the last decade in this region. The deep convection event of 2008 is evident in both the temperature and salinity fields. The Argo composite indicates that the winter of 2011 was similar to the preceding winter with very limited convection (mixed layer depths might fluctuate between 200 and 400 m). Convection reached depths of down to 1400 m in 2012, which is clearly shown by temperature and salinity data from Argo floats. The salinity in the top 200 m in 2012 was the lowest since 2003, particularly in the top 50 m. Convection also occurred in the winter of 2013, but it was not as deep as in the previous year, and was mostly limited to the top 1000 m. The situation changed quite significantly in 2014. Wintertime cooling that triggered convective mixing throughout the top 1600 m layer of the water column in the central region of the Labrador Sea. The high NAO event in 2015 also clearly showed an impact on convection in the Labrador Sea, with winter deep convection reaching 1800 m.

The hydrographic sampling of the AR7W line, conducted in May of 2015 (Figure 8), confirmed that the convective mixing that took place in the previous winter reached depths of 1800 m depth and possibly deeper, consistent with the analysis based on Argo float profiles (Figure 7). The 2015 LSW (Labrador Sea Water) was mostly colder than 2014 LSW, but the difference in salinity between 2014 and 2015 was not obvious (Figure 8), although the 2015 LSW in the far eastern portion was slightly saltier. It seems possible that the source of convection was limited in area, but that convection was prolonged in duration so that the newly-mixed water spread from its local source out and across the Labrador Sea. The cold and less saline water mass layer below 3000 m is clearly shown in the hydrographic data from this survey.

Other than being the main factor of interannual variability of the intermediate layer throughout the North Atlantic, wintertime convection in the Labrador Sea is a key process in the Atlantic Meridional Overturning

Circulation (AMOC), and the Labrador Sea is one of the few areas in the global ocean where surface water is exchanged with the deep ocean. It also has an important role in biogeochemical cycling in the Labrador Sea, and strong convection enhances the entrainment of gases such as oxygen and carbon dioxide into the deep water from the atmosphere, as well as from surface freshwater.

Total Inorganic Carbon and pH

About one quarter of carbon dioxide (CO_2) released by human activities (anthropogenic CO_2, mainly due to fossil fuel combustion) has been taken up by the oceans, altering the basic ocean chemistry, specifically the marine carbonate system. The dissolution of anthropogenic CO_2 has decreased the ocean pH by 0.1 units over the past 200 years, corresponding to a 30% increase in acidity (Caldeira and Wickett, 2003). If global emissions of CO_2 continue at their present rate, the ocean pH is predicted to fall an additional 0.3 units by 2100. The oceans have not experienced such a rapid pH decrease (ocean acidification) or one of such great a magnitude for at least 20 million years (Feely et al., 2004), raising serious concerns about the ability of marine ecosystems to adapt. The major impact of decreasing pH will be felt by organisms that form calcium carbonate ($CaCO_3$) shells and skeletons, because rising acidity increases the solubility of $CaCO_3$. Since $CaCO_3$ shells and skeletons are naturally more soluble at lower temperatures and higher pressures, high latitude and deep water ecosystems will be more vulnerable to the added stress of ocean acidification. Furthermore, rapid environmental changes such as retreating ice extent and enhanced hydrological cycles may amplify these problems.

Arctic outflow and the local uptake of anthropogenic CO_2 in the deep convection region of the Labrador Sea are major controlling mechanisms for the state of ocean acidification in the Northwest Atlantic. The Arctic water inflows into the highly productive regions in the Northwest Atlantic, which have important commercial fisheries, make these regions more susceptible to future ocean acidification than other regions (Azetsu-Scott et al., 2010). The Labrador Sea is the site of a strong “solubility pump”; anthropogenic CO_2 sequestration from the atmosphere is transported to the deep ocean by chemical and physical processes. In the newly ventilated Labrador Sea water (NV-LSW), which ranges between 150-500 m deep for stations in the central part of the Labrador Basin, DIC (Dissolved Inorganic Carbon) increased by 16.75 $\mu mol\ kg^{-1}$ from 1996 to 2015, reaching a maximum of 2162.3 $\mu mol\ kg^{-1}$, due to the local uptake of anthropogenic CO_2 (Figure 9). As a result, the pH decreased by 0.07 units (in the total pH scale) during the same period (Figure 9) representing a decline rate of 0.003 y^{-1}, higher than the global average of 0.002 y^{-1}. Despite the slight differences observed in the metrics over the last few years, observed trends between 1996 to 2015 remain highly significant with R^2 explaining respectively 87% and 79% of the variance for DIC and pH. Ocean acidification influences the capacity of the ocean to take up CO_2 from the atmosphere. Continued monitoring of the chemical state and investigation of biological responses to ocean acidification in the Northwest Atlantic are urgently needed.

Transient tracers CFC-12 and SF6

During the second half of the twentieth century, the atmospheric burden of chlorofluorocarbons (CFCs) increased steadily due mainly to their widespread use as refrigerants and aerosol propellants. The invasive atmospheric flux of these mostly inert gases provides an excellent record of ocean circulation, and profiles of dissolved CFC-12 concentration have been measured annually along the AR7W line since 1991. As a consequence of restrictions on the manufacture and use of ozone depleting substances introduced in 1989, the atmospheric mixing ratio of CFC-12 has been in decline since 2003 and so it is becoming less useful as a tracer of very recent ventilation. Measurements of an alternative transient tracer, sulphur hexafluoride (SF6), were introduced in 2011. There has been a rapid near-linear increase in atmospheric SF6 since around 1980 and dissolved concentration profiles show enhanced structure in recently ventilated water compared with CFC-12. Figure 10 shows dissolved concentrations of SF6 and CFC-12 along the AR7W line in May 2015. Figure 11 shows mean concentrations of CFC-12 and SF6 in newly-ventilated Labrador Sea Water (150-500 m depth in Labrador Sea Central Basin) from 1991 to present.

Ocean colour from remote sensing

Ocean colour, as an indicator of sea surface chlorophyll-*a* concentration (SSC), is derived from observations made by the Moderate Resolution Imaging Spectroradiometer (MODIS) aboard the Aqua Earth Observing System satellite between 2003 and 2012 and by the Visible Infrared Imaging Radiometer Suite (VIIRS) since 2013. Remotely-sensed images of ocean colour for the Labrador Sea are composited on a 2-week basis from the beginning of March to the end of October each year. Between November and February, the data are too sparse to be useful. From these composites, ocean colour data are extracted from 511 pixels comprising the AR7W transect. A biweekly climatology of SSC constructed from the time series of ocean colour from 2003 to 2015 (Figure 12), and fitted with a Gaussian function to extract the principals blooms metrics following Zhai et al (2011) indicates that the annual phytoplankton spring bloom starts earlier on the central Labrador basin and Greenland Shelf (mid-April to early June) compared to the Labrador Shelf (early May to late June). However in 2015 timing of the bloom was particularly early in the central basin, starting mid-April, one of the earliest starting dates since 2002. While brief, at only 49 days in duration, this bloom was unusually intense with the highest amplitude ever recorded for the region (over 5mg m^{-3}) and giving a seasonally integrated value among the highest ever seen. Greenland shelf characteristics followed the same pattern, while the Labrador Shelf bloom metrics were all average for the region. Within the two-dimensional spatial regional boxes defined by Harrison and Li (2008), the SSCs averaged over the period from March to October 2015 were 0.62 mg m^{-3} on the Labrador Shelf, 3.20 mg m^{-3} in the central Labrador Basin, and 1.61 mg m^{-3} on the Greenland Shelf (Figure 13).

Phytoplankton

Upper ocean (z<100m) phytoplankton sampled on AR7W in the spring and early summer between 1994 and 2013 shows region-specific characteristics (Li and Harrison 2014). The Greenland Shelf is a region with high concentrations of chlorophyll-*a* and nanophytoplankton, but low concentrations of picophytoplankton. Conversely, the central Labrador Basin is a region with lower concentrations of chlorophyll-*a* and nanophytoplankton, but high concentrations of picophytoplankton and bacteria. The Labrador Shelf has the lowest concentrations of chlorophyll-*a* and nanophytoplankton, but intermediate concentrations of picophytoplankton. During May 2015, concentrations of chlorophyll-*a* in the central basin region appeared to be among the highest regionally-specific values ever recorded (Figure 14). The Greenland Shelf/slope region values were also amongst the highest recorded, while the Labrador shelf/slope region values were average. *Phaeocystis* sp. colonies apparently dominated the widespread bloom in the central basin; they were easily identifiable by the large amounts of mucilage they produce, which accumulated on filters, leading to slow filtration rates, and clogged plankton nets. Upper ocean (z<100m) temperatures were also at the low end of the record values with the exception of the Greenland Shelf that was around average. For program resource reasons, the time series of picophytoplankton, nanophytoplankton, and bacterial counts were discontinued in 2013.

Mesozooplankton

One species of copepod, *Calanus finmarchicus*, dominates the mesozooplankton biomass in the central region of the Labrador Sea, while on the shelves *C. finmarchicus*, *C. glacialis* and *C. hyperboreus* each contribute about one third (Head et al. 2003). *C. finmarchicus* abundances show regional variations that are generally consistent from year-to-year and are related to regional differences in the timing of the life-cycle events, which are themselves influenced by environmental conditions. On the Labrador Shelf, *C. finmarchicus* abundances are generally relatively low in spring (Figure 14), as was the case in 2015. In spring, populations here generally have few young stages from the new years' generations, but their abundances increase in summer when they dominate the populations There was no significant trend in springtime abundance of *C. finmarchicus* between 1996 and 2015 on the Labrador Shelf. In the Central Labrador Sea, total *C. finmarchicus* abundance is generally relatively low in spring and summer, with a low proportion of young stages; one exception being the summer of 1995, when young stages were dominant and total abundance was relatively high. There was no trend in springtime total abundance between 1996 and 2015 in the Central Labrador Sea and the abundance in 2015 was near the low values seen in previous springs. *C. finmarchicus* abundances are generally higher in the eastern Labrador Sea than farther west in spring, because the spring bloom starts earlier here, which leads to earlier reproduction in *C. finmarchicus*. Abundances are generally higher here in summer than in spring, with the highest concentration of all occurring in spring 2006. The abundance in 2015 was at the low end of the range of values seen in previous springs, and there was no trend in springtime abundance between 1996 and 2014. PDI% represents the proportion of Copepodite C1 to C3 over the entire population express in percent and shows the proportion of recently produced younger stages within each region. In all three regions the PDIs were around the average values seen since 1995 (Figure 14).

Mesozooplankton organisms were regrouped 4 large classes; *Calanus* spp., *Pseudocalanus* spp., "other copepods" and "non-copepods". In general, abundances have been lower than usual during the last three years, one exception being in 2014 on the Greenland shelf/slope. However the large phytoplankton bloom, mainly composed of *Phaeocystis* sp. that stretched from the Greenland Shelf in the east all the way to the base of the Labrador slope in the west (station 11) undoubtedly impaired the filtration rates of the plankton nets causing more or less severe clogging at almost every station. Abundance estimates were corrected for the lower filtered volumes using the flowmeter readings, but even so, the vertical sampling of the water column was certainly not evenly distributed between100 m to the surface (Figure 15).

Continuous Plankton Recorder (CPR)

The Continuous Plankton Recorder (CPR) is an instrument that is towed by commercial ships that collects plankton at a depth of ~7 m on a long continuous ribbon of silk (~260 µm mesh). The position on the silk corresponds to the location of the different sampling stations. CPR data are analysed to detect changes in indices of phytoplankton concentration (colour and relative numerical abundance) and zooplankton relative abundance for different months, years and/or decades in the northwest Atlantic. The indices indicate relative changes in concentration (Richardson et al. 2006). The sampling methods from the first surveys in the northwest Atlantic (1957 for the sub-polar gyre, 1960 for the Canadian continental shelf) to the present are exactly the same so that valid comparisons can be made between months, years and decades. CPR data collected from January to December 2014 were made available in January 2016 to add to the DFO data archive.

The tow routes between Reykjavik and the Gulf of Maine are divided into eight regions: the Western Scotian Shelf (WSS), the Eastern Scotian Shelf (ESS), the South Newfoundland Shelf (SNS), the Newfoundland Shelf (NS) and four regions in the NW Atlantic sub-polar gyre, divided into 5 degree of longitude bins (Fig. 16). In this report a broad-scale comparison is presented for CPR data collected in all regions and all sampling decades. More detailed analyses for the Scotian Shelf and Newfoundland Shelf regions are presented in the annual AZMP Reports from the Maritimes and Newfoundland Regions. These latter reports concentrate on data collected since 1992, since these are comparable to AZMP survey results, which date back to 1999.

Monthly average abundances ($\log_{10}(N+1)$ transformed for all but PCI[1]) were calculated for 15 CPR taxa by averaging values for all individual samples collected within each region for each month and year. These regional monthly average abundances were then averaged by month for samples collected within each decade prior to 2009, (i.e. 1960-1969, 1970-1979, 1980-1989, 1990-1999 and 2000-2009) to give decadal monthly average abundances, which were then averaged for each decade to give decadal annual average abundances. During the 1980s sampling was too infrequent to calculate decadal annual average abundances, except for the three regions between 30 and 45^{o}W, and even in these regions there was no sampling in January or December. The averages of the monthly values for the 1970s and 1990s were used to fill in these missing months, however, so that decadal annual average abundances could be calculated. The averages of the decadal annual average abundances over the 4 or 5 sampling decades represent the climatological average annual abundances. Four-year annual average abundances were calculated for 2010-2013, using the 4-year monthly averages, and annual average abundances were calculated for 2014, where possible. According to the protocol used here, annual averages for individual years can only be calculated if there was sampling in more than 8 months, with no gaps of more than 2 consecutive months (linear interpolation being used to fill in for missing months). These criteria were met in 7 regions in 2014, for which there were 0-3 missing months, with no 2 or 3 month gaps. No annual average abundances could be calculated for the SNS region in 2014, since there was sampling in only 6 months and a 5 month gap.

[1] PCI – Phytoplankton colour index, a semi-quantitative measure of total phytoplankton abundance.

Standardized abundance anomalies were calculated for the decadal (1960s, 1970s, 1980s, 1990s, 2000s), four-year (2010-2013) and annual (2014) average abundances, by subtracting the climatological average annual abundances for each time period, and by dividing the differences by the standard deviations calculated for the annual average abundances available for the individual years between 1992 and 2009. Sampling coverage was good everywhere over this period, so that annual averages could be calculated for 13-15 individual years in all regions. The underlying assumption of this approach to the calculation of the standardized abundance anomalies is that inter-annual variability was similar for all decades. This assumption was found to be reasonable for the 1960-1970s in the four regions of the sub-polar gyre, decades for which annual average abundances and standard deviations could be calculated for 15 individual years. As well, it was not inconsistent with results for the shelf regions, where annual averages over the same decades could be calculated for only 2-6 years.

The phytoplankton colour index (PCI).

Climatological annual PCI values (1960-2009) are highest in the two Newfoundland Shelf regions (NS, SNS), intermediate on the Scotian Shelf (WSS, ESS) and lower in the regions between 25 and 45˚W (Fig. 17). In the sub-polar gyre decadal average annual PCI values increased in all regions between the 1970s and 1990s and increased further thereafter, reaching record high values in 2014. In shelf regions PCI values peaked in the 1990s, dipped in the 2000s and 2010-2013, and increased in 2014.

Diatoms.

Climatological annual abundances for diatoms are highest on the NS, intermediate in the SNS and ESS regions and lower in the WSS and sub-polar gyre regions (Fig. 17). Decadal average annual abundances increased everywhere after the 1970s, with highest values in the 1990s (ESS) or 2000s (other regions). In 2010-2013 abundances increased in the sub-polar gyre and decreased in shelf regions, while in 2014 they were near (25-40˚W, WSS), higher (NS, 40-45˚W) or lower (ESS) than average.

Dinoflagellates

Climatological annual abundances for dinoflagellates are higher in shelf regions than in the sub-polar gyre. Dinoflagellate abundances increased after the 1970s with highest values in the 1990s (ESS, WSS) or 2000s (other regions) (Fig. 17). In 2010-2013, dinoflagellate abundances decreased (3 regions east of 40˚W), increased (WSS) or did not change (4 other regions). In 2014 the downward trend continued in the 3 eastern regions and the upward trend continued on the WSS, while in the NS and 40-45˚W regions dinoflagellate abundances remained at the relatively high 2010-2013 levels.

Calanus I-IV

Climatological annual abundances for *Calanus* I-IV (mostly *Calanus finmarchicus*) are similar in most regions, but higher on the NS (Fig. 18). In the sub-polar gyre abundances increased over the decades, peaking in 2010-2013 and decreasing in 2014. For shelf regions decadal abundance anomalies have decreased since the 1970s, except for the WSS, which shows the opposite trend (highest in the 2000s). In 2010-2013 *Calanus* I-IV abundances were close to average (NS, SNS, WSS) or lower than average (ESS), while in 2014 they were close to average.

Calanus finmarchicus V-VI

Climatological annual average abundances for *C. finmarchicus* V-VI increase slightly from east to west across the sub-polar gyre, decrease on the SNS and increase slightly farther west (Fig. 18). In the 4 sub-polar gyre regions abundance anomalies have been close to average throughout the entire sampling period. For the NS and SNS abundance anomalies were close to average until 2013, but increased on the NS in 2014. On the Scotian Shelf abundance anomalies were relatively high in the 1970s and since then have been close to average on the WSS and lower than average on the ESS, especially in 2014.

Calanus glacialis V-VI

Climatological annual abundances for *C. glacialis* are low in most regions, but higher on the NS than elsewhere (Fig. 18). Decadal abundance anomalies increased slightly in all regions over the decades to maximum values in the 1990s (NS) or 2000s (other regions). In 2010-2013, *C. glacialis* abundance anomalies were close to average in all regions and in 2014 they remained near average everywhere, except for an increase on the NS.

Calanus hyperboreus III-VI

Climatological annual abundances for *C. hyperboreus* are very low in most regions, but higher on the NS than elsewhere (Fig. 18). In most regions decadal abundance anomalies were close to average between the 1960s and 2000s, but in the 25-30˚W region, the abundance anomaly was high in the 1970s, decreasing thereafter, with lowest values in 2010-2013 and 2014. Elsewhere abundance anomalies have remained close to average since the 2000s, although the WSS has shown an upward trend, with a relatively high value in 2014.

Small copepod taxa (Copepod nauplii, *Paracalanus/Pseudocalanus*, *Oithona* spp.)

The climatological abundances of the three small copepod groups are higher in shelf regions than in the sub-polar gyre (Fig. 19). In the sub-polar gyre, decadal annual abundance anomalies for copepod nauplii and *Paracalanus/Pseudocalanus* have been higher since the 1990s than they were in previous decades, but both taxa decreased slightly in abundance in 2014. For shelf regions decadal annual abundance anomalies for copepod nauplii increased between the 1970s and 1990s and remained high (NS) or dropped to near average values in the 2000s and 2010-2013, increasing (NS, WSS) or decreasing (ESS) in 2014. *Paracalanus/Pseudocalanus* abundance anomalies in shelf regions have generally been near average, but unusually high on the NS in the 1960s and low in the SNS, ESS and WSS regions during 2010-2013 and/or 2014. Decadal annual abundances for *Oithona* spp. were generally close to average throughout all regions until the 2000s: thereafter they remained close to average in most regions, but were higher than average in the 40-45˚W region in 2010-2013 and on the NS in 2014.

Macrozooplankton

Climatological annual abundances for euphausiids and hyperiid amphipods are mainly higher in the deep ocean regions of the sub-polar gyre and are highest in the 40-45˚W region (Fig. 20). In the sub-polar gyre euphausiid decadal abundance anomalies were generally close to average until the 2000s, but since then have been lower than average. In shelf regions euphausiid abundance anomalies have shown a downward trend since the 1970s, but with an increase to near average levels on the NS in 2014. Abundance anomalies for hyperiid amphipods increased in all regions in the 1990s compared with previous decades, although only for the NS and SNS regions were values ever very different from average during the entire 1960-2009 period, with low values on the SNS (1960s) and high values on the NS and SNS (1990s). In 2010-2013 abundance anomalies increased to higher than average values in 5 regions (2 sub-polar gyre, 3 shelf regions), while in 2014 they were lower than average in 2 sub-polar gyre regions and much higher than average in shelf regions.

Acid-sensitive taxa

Coccolithphores, phytoplankton that are covered with calcite scales, and foraminifera (forams) whose shell composition includes calcium carbonate, have been counted in CPR samples only since 1991. Coccolithophores are generally less abundant on the NS and Scotian Shelf than elsewhere and forams are more abundant in the sub-polar gyre than in shelf regions (Fig. 21). Changes in coccolithophore abundance may be linked to changes in stratification (Raitsos et al. 2006). Both taxa were generally more abundant in 2010-2013 than before and both remained at high levels in 2014 in the regions between 40^{o}W and the ESS. Elsewhere abundance anomalies for both taxa were generally near average in 2014, except for high values for coccolithphores in the 30-35^{o}W region and for forams on the WSS. Pteropods of the genus *Limacina* have shells that are composed of aragonite, which is a form of calcium carbonate that is especially sensitive to dissolution at low pH. Climatological annual abundances for *Limacina* show a more-or-less flat distribution across all regions. Over the decades *Limacina* abundance anomalies have generally been close to average, but in 2010-2013 they were higher than average in the NS and WSS regions, remaining high on the NS in 2014. Elsewhere abundance anomalies were close to average in 2014.

Summary

The winter convective overturning in the central Labrador Sea reached a maximum depth of 1850 m in 2015 following a maximum of 1700 m in 2014. This is the deepest since 1994, when a record depth of 2400 m was observed. The resulting Labrador Sea Water year class is one of the largest in two decades and led to the increased uptake and increased concentrations of atmospheric gases (dissolved oxygen, anthropogenic gases, and carbon dioxide) that spread over the entire water mass, reaching as deep as 1900 m in some places. Changes in the phase of the NAO are continuing to drive the inter-annual variability in heat content in the Labrador Sea. Since 2012 the NAO has mostly been in a high positive phase, which is associated with strong winter atmospheric cooling, leading to accumulated surface heat loss and deep convection. It is also contributing to the decadal-scale variability in deep-water properties and transport across the sub-polar North Atlantic and potentially in the AMOC. Yearly and seasonal remotely sensed averages anomaly time series of sea surface temperature (SST) demonstrate this are shown in Figure 22).

Initiation of the spring bloom occurred earlier than usual on the Greenland Shelf and in the Central basin, in the first week of May. The spring bloom was generally short but very intense particularly in the Central basin. It resulted in normal or above normal seasonal average chlorophyll concentrations for 2015 in the three Labrador Sea regions (Figure 23). Mesozooplankton was generally low in abundance for a third consecutive year (Figure 23).

Acknowledgements

We would like to thank Blair Greenan for his helpful comments and suggestions. The NCEP Reanalysis data were provided by the NOAA-CIRES Climate Diagnostics Center, Boulder, Colorado, USA. The sea ice concentration anomaly data are the US National Snow and Ice Data Center. Thanks also goes to Ingrid Peterson for the help in ice extent data extraction and handling. The authors wish to thank the many staff and associates at BIO have contributed to the AZOMP mission which was carried out by the Ocean and Ecosystem Sciences Division in 2015. These efforts, together with those of the officers and crew of CCGS *Hudson*, are gratefully acknowledged.

References

Azetsu-Scott, K., A. Clarke, K. Falkner, J. Hamilton, E. P. Jones, C. Lee, B. Petrie, S. Prinsenberg, M. Starr and P. Yeats (2010), Calcium Carbonate Saturation States in the waters of the Canadian Arctic Archipelago and the Labrador Sea, 115, C11021, doi:10.1029/2009JC005917 Journal of Geophysical Research.

Barnston, A. G., and R. E. Livezey (1987), Classification, seasonality and persistence of low-frequency atmospheric circulation patterns. Mon. Wea. Rev., 115, 1083-1126.

Caldeira, K., and M. E. Wickett (2003), Anthropogenic carbon and ocean pH, Nature, 425, 365

Climate Prediction Center (2010), NOAA/National Weather Service, National Centers for Environmental Prediction. Camp Springs, MA. http://www.cpc.noaa.gov/products/precip/CWlink/daily_ao_index/ao.shtml#publication

Egge, J., and Aksnes, D.L. (1992), Silicate as regulating nutrient in phytoplankton competition. Mar. Ecol. Prog. Ser. **83**(2-3): 281–289. doi: 10.3354/meps083281.

Fetterer, F., K. Knowles, W. Meier, and M. Savoie (2002), updated 2011. Sea ice index. Boulder, CO: National Snow and Ice Data Center. Digital media.

Feely, R. A., C. L. Sabine, K. Lee, W. Berelson, J. Kleypas, V. J. Fabry,and F. J. Millero (2004), Impact of anthropogenic CO_2 on the $CaCO_3$system in the oceans, Science, 305, 362–366.

Harrison, W.G. and W.K.W. Li (2008), Phytoplankton growth and regulation in the Labrador Sea: light and nutrient limitation. J. Northwest. Atl. Fish. 39:71-82.

Hauser, T., Demirov, E., Zhu, J. and I Yashayaev (2015), North Atlantic atmospheric and ocean inter-annual variability over the past fifty years – Dominant patterns and decadal shifts. Progress in Oceanography, Volume 132, March 2015, Pages 197–219

Head, E.J.H., Harris, L.R and I Yashayaev. (2003), Distributions of *Calanus* spp. and other mesozooplankton in the Labrador Sea in relation to hydrography in spring and early summer (1995-2000). Prog. Oceanogr. 59: 1-30

Hurrell, J. W. (1995), Decadal trends in the North Atlantic Oscillation: Regional temperatures and precipitation. Science, 269, 676-679.

Josey, S., J. Grist, D. Kieke, I. Yashayaev, and L. Yu (2015), Sidebar: Extraordinary ocean cooling and new dense water formation in the North Atlantic [in "State of the Climate 2014"], Bull. Amer. Meteor. Soc.

Kalnay, E., M. Kanamitsu, R. Kistler, W. Collins, D. Deaven, L. Gandin, M. Iredell, S. Saha, G. White, J. Woollen, Y. Zhu, M. Chelliah, W. Ebisuzaki, W. Higgins, J. Janowiak, K.C. Mo, C. Ropelewski, J. Wang, A. Leetmaa, R. Reynolds, R. Jenne, and D. Joseph (1996), The NCEP/NCAR 40-Year Reanalysis Project., Bull. Amer. Meteor. Soc., 77, No. 3, 437-470.

Li, W.K.W. and W.G. Harisson, 2014, The state of phytoplankton and bacterioplankton and bacterioplankton in the Labrador Sea: Atlantic Zone Off-Shelf Monitoring Program 1994-2013. Can. Tech. Rep. Hydrogr. Ocean. Sci. 302:xviii+181p.

Raitsos, D.E., Lavender, S.J., Pradhan, Y., Tyrrell, T., Reid, P.C., Edwards, M. (2006), Coccolithophore bloom size variation in response to the regional environment of the subarctic North Atlantic. Limnol. Oceanogr. 51: 2122-2130.

Rey, F. (2012), Declining silicate concentrations in the Norwegian and Barents Seas. ICES J. Mar. Sci. J. Cons. **69**(2): 208–212

Richardson, A.J., Walne, John, A.W.G., Jonas, T.D., Lindley, J.A., Sims, D.W., Stevens, D. and M. Witt, (2006), Using continuous plankton recorder data. Prog. Oceanogr. 68: 27-74.

Visbeck, M.H., J.W. Hurrell, L. Polvani and H.M. Cullen (2001), The North Atlantic Oscillation: Past, Present and Future. Proc. Nat. Acad. Sci., 98, 12876-12877 doi: 10.1073/pnas.231391598

Yashayaev, I. (2007), Hydrographic changes in the Labrador Sea, 1960-2005, Progress in Oceanography, 73, 242-276.

Yashayaev, I., and J.W.Loder (2009), Enhanced production of Labrador Sea Water in 2008. Geophys. Res. Lett., 36: L01606, doi:10.1029/2008GL036162.

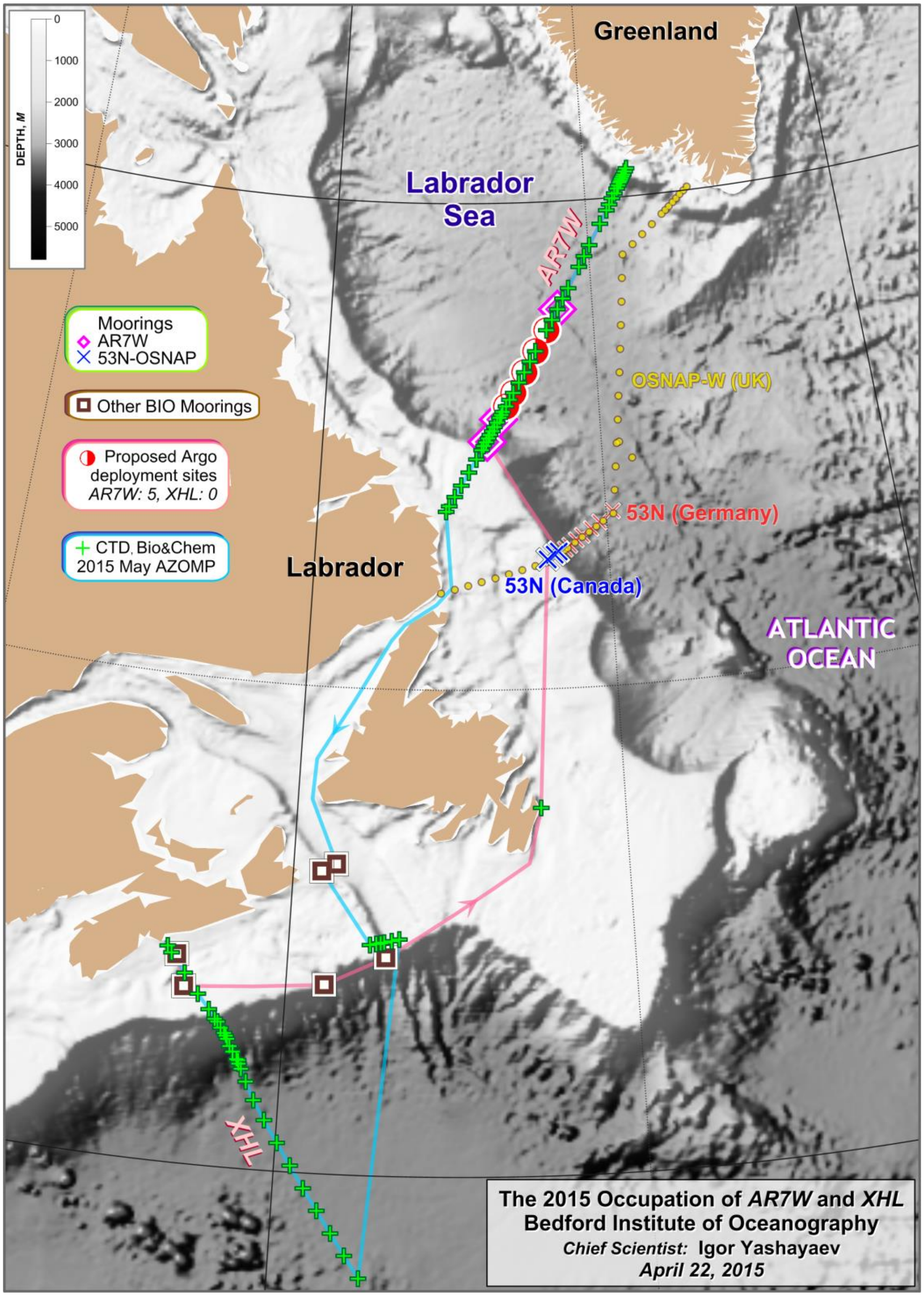

Fig. 1. Schematic of the Labrador Sea component of the DFO Atlantic Zone Offshore Monitoring Program (AZOMP). Standard stations along the sections are shown as green plus signs, mooring sites are indicate by purple open lozenge and blue cross (OSNAP), and circles indicate the location of biology and VITALS casts. Location of Argo profiler deployments are indicated by the red/white circles.

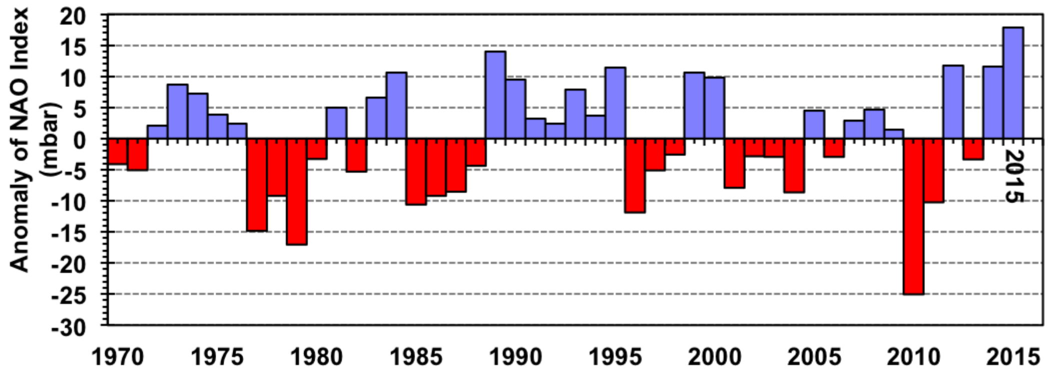

Fig. 2. Average Sea Level Pressure for Dec, Jan, Feb in mbar (Winter North Atlantic Oscillation Index)

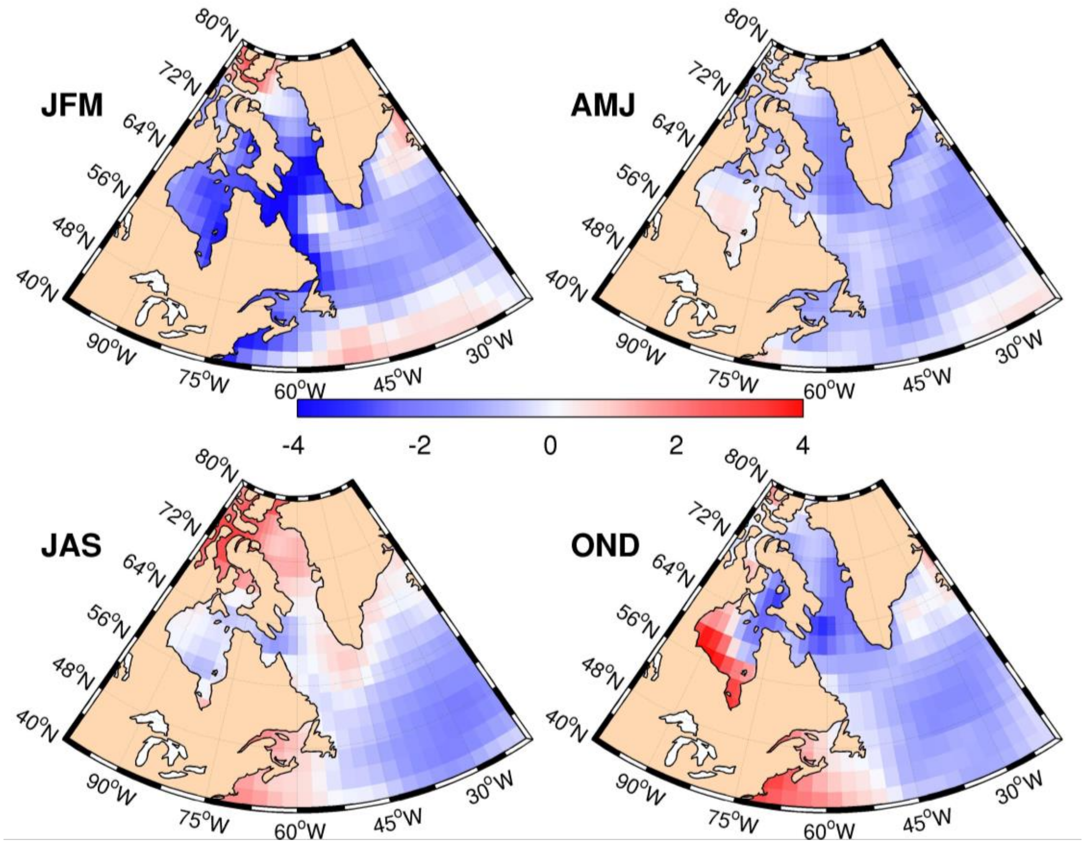

Fig 3. Surface air temperature anomaly for winter, spring, summer and fall periods in 2015 as derived from NCEP/NCAR reanalysis. http://www.esrl.noaa.gov/psd/

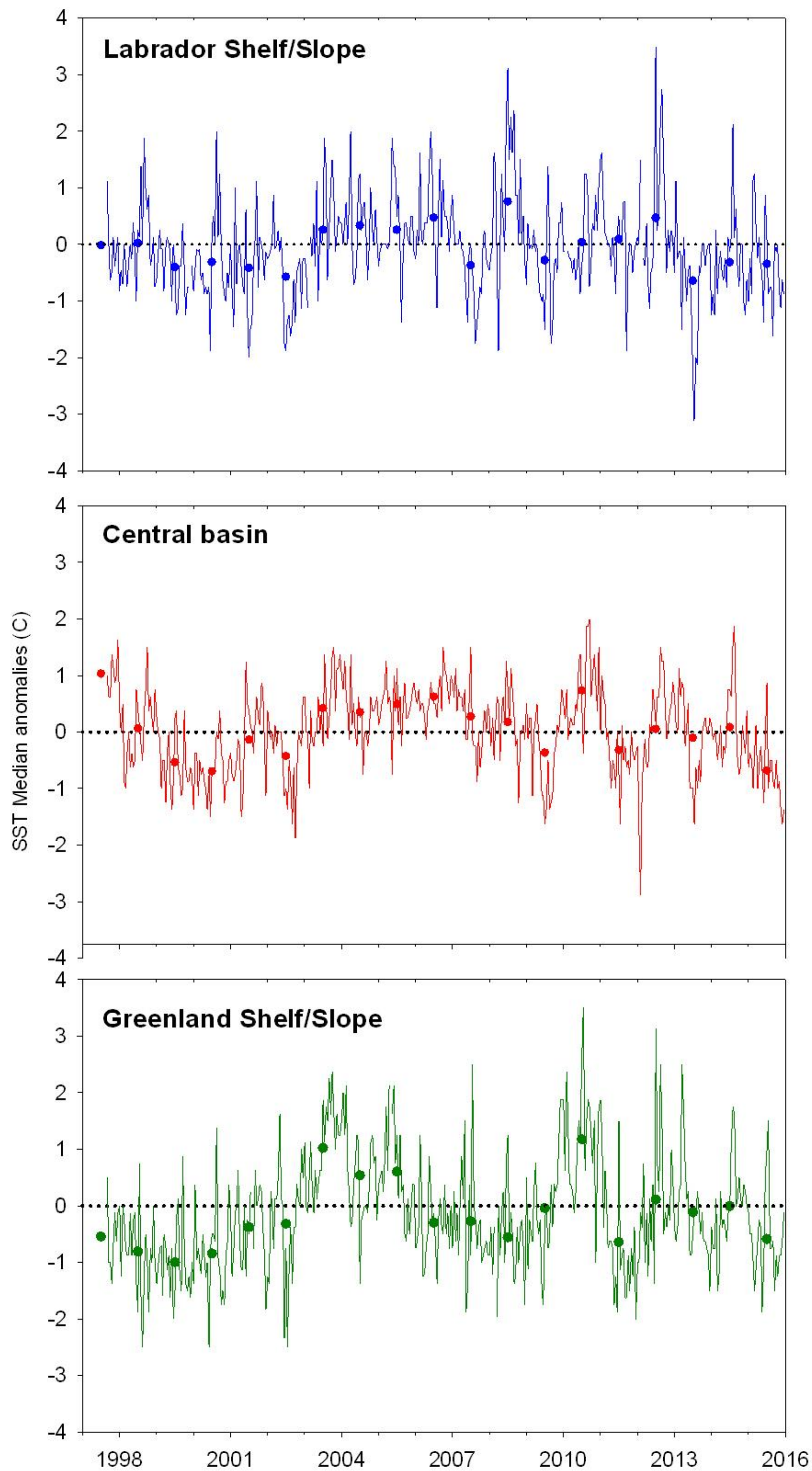

Fig. 4. Sea surface temperature median anomalies derived from NOAA AVHRR (reference period 1997-2010) in the Labrador shelf/slope in blue, the Central basin and the Circles represent the annual average anomalies.

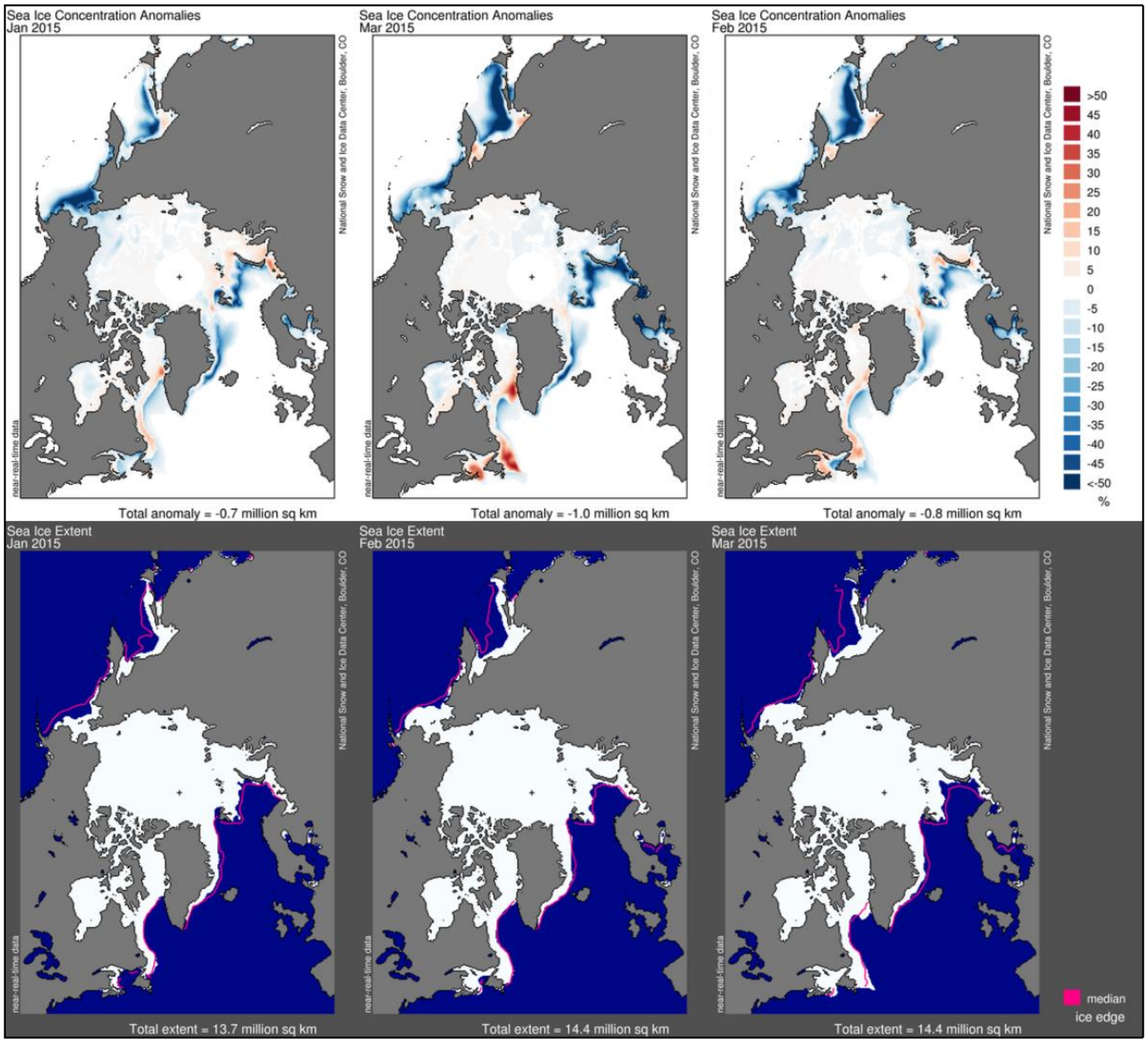

Fig. 5. Sea ice concentration anomalies (A) and sea ice extent (B) for Jan-Mar 2015 as derived by the US National Snow and Ice Data Center (reference period 1979-2000) http://nsidc.org/

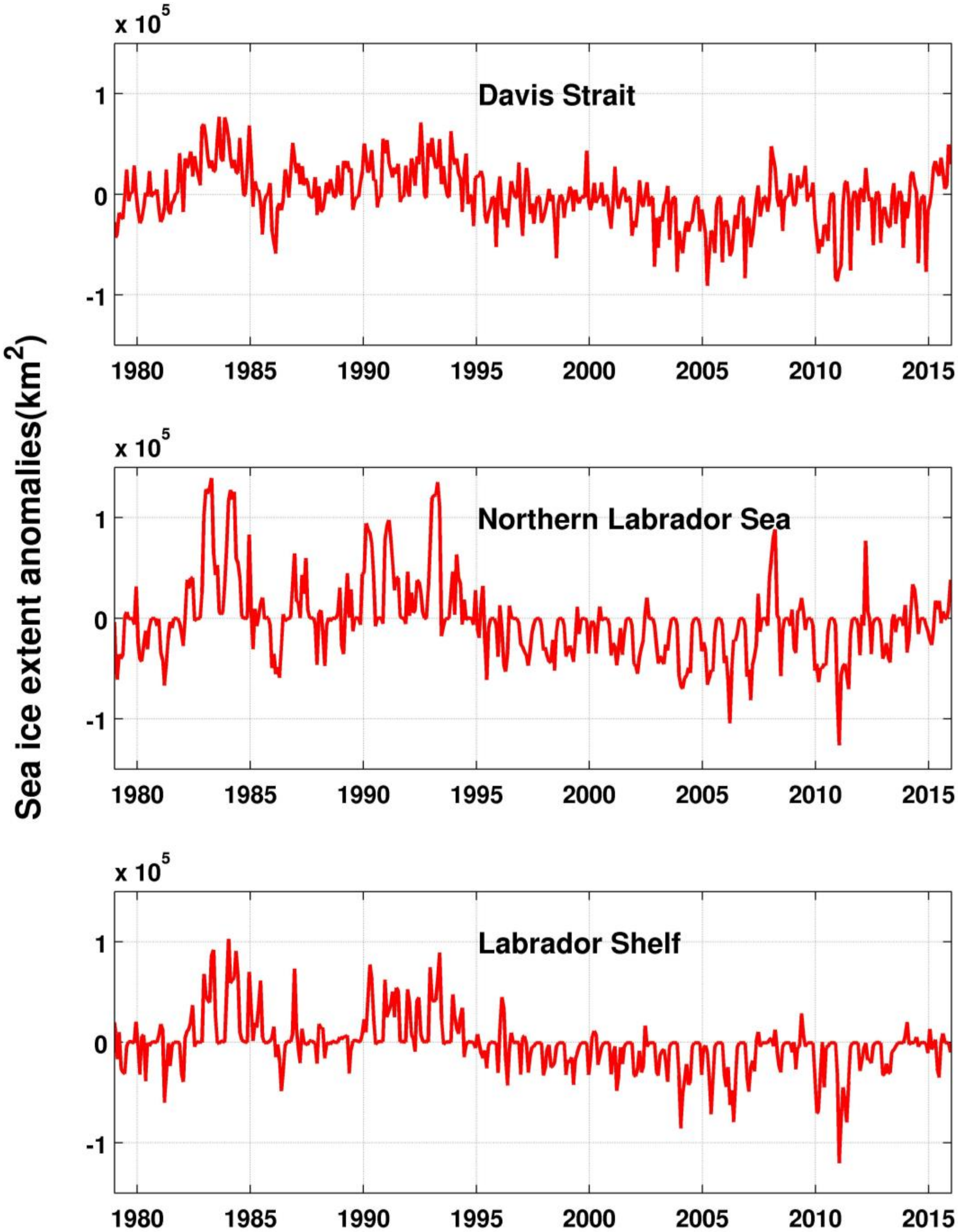

Fig. 6. The computed monthly sea ice extent anomalies for Davis Strait area, northern Labrador Sea, and Labrador Shelf, based on ice concentration data from the US National Snow and Ice Data Center (reference period 1981-2010). http://nsidc.org/data/

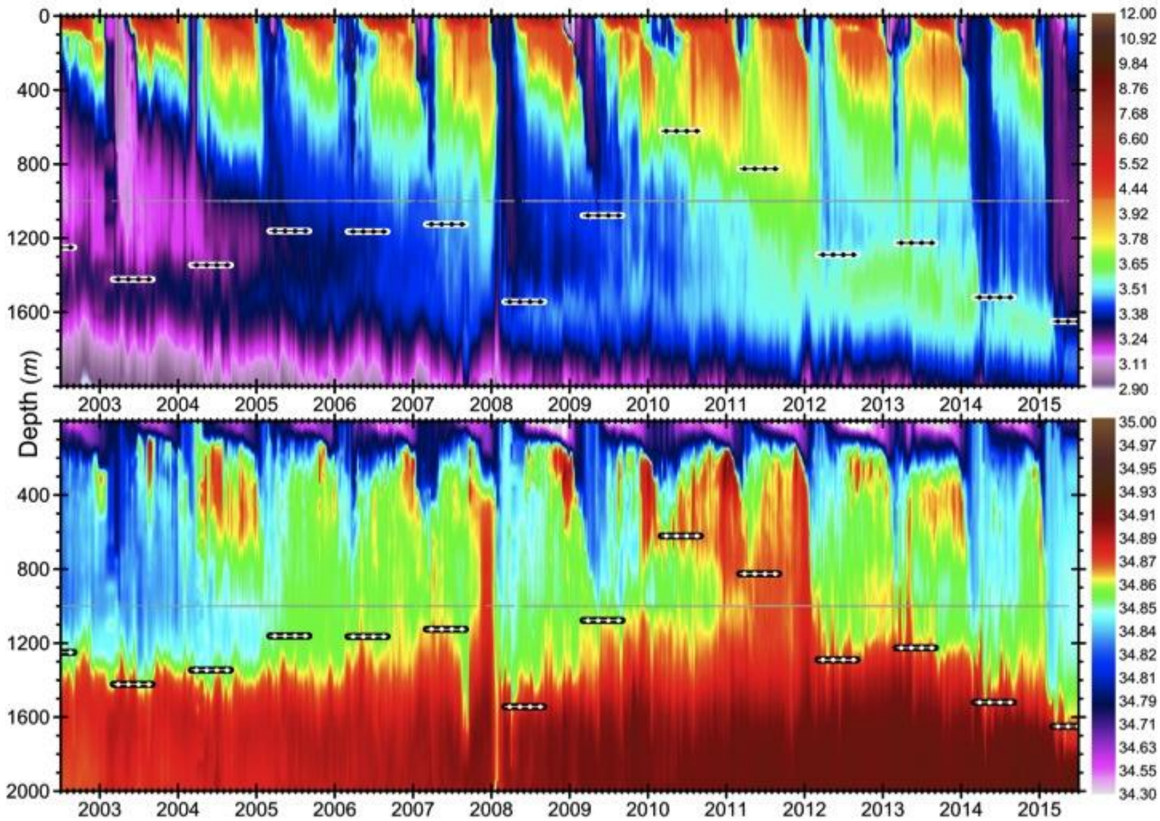

Fig. 7. Potential temperature (top) and Salinity (bottom) from Argo drifters in the Labrador Sea. The winter deep convection event of 2008, 2012, 2014 and 2015 have clearly extend beyond 1400m. Convection was limited to a depth of about 200 m in the winters of 2010 and 2011

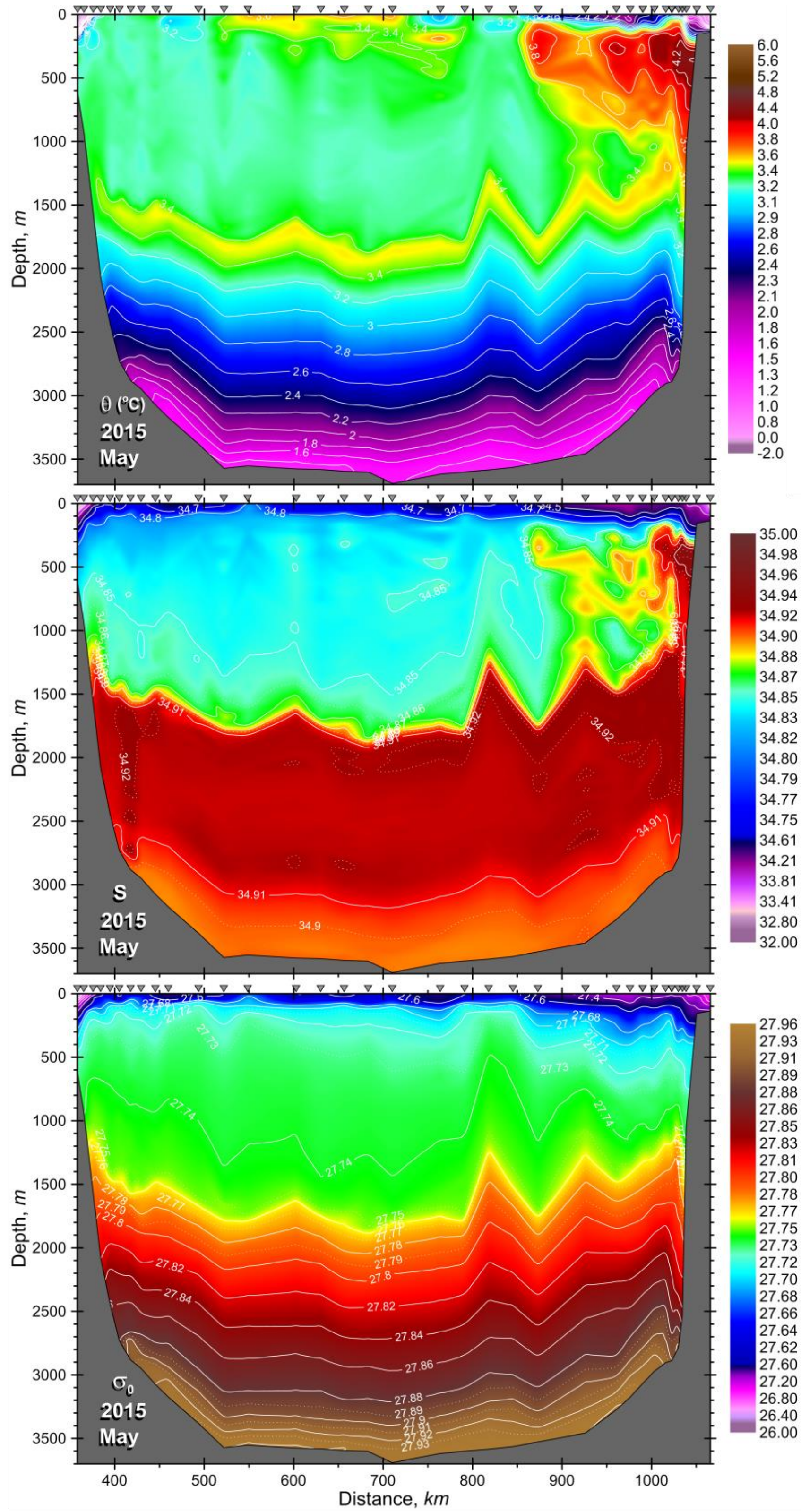

Fig. 8. Labrador Sea (AR7W Section) potential temperature (top), salinity (middle) and potential density (bottom).

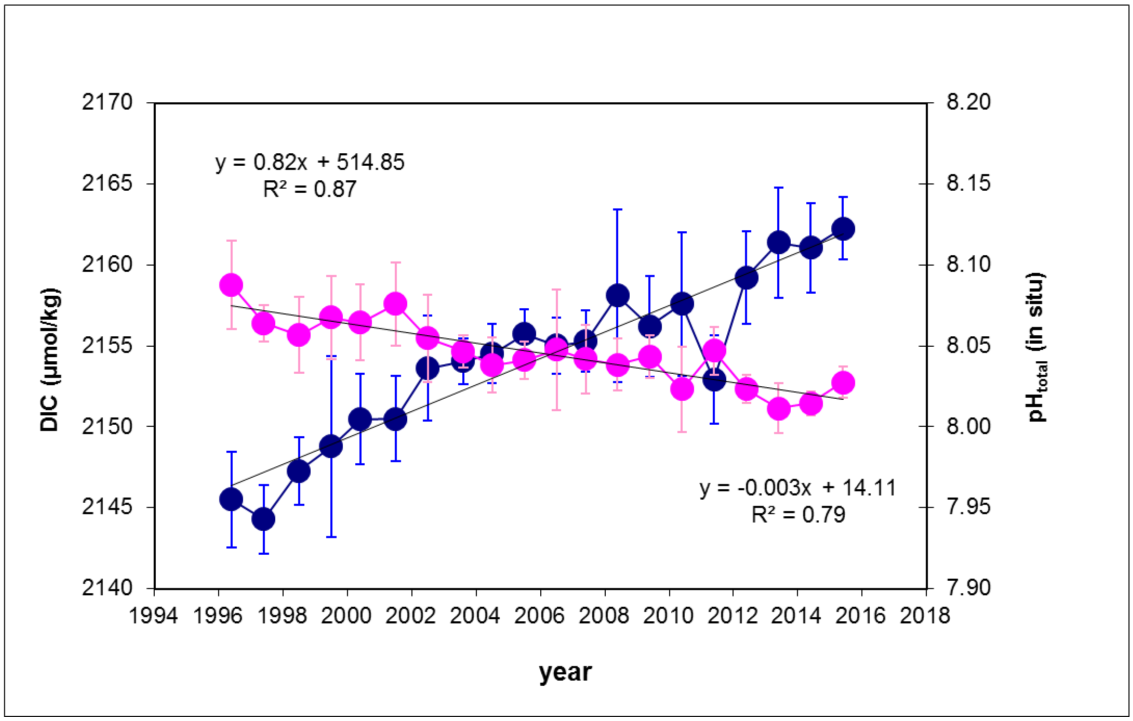

Fig. 9. Time series of total inorganic carbon (TIC) and PH, top panel for TIC, bottom panel from PH. TIC and PH in in the 150–500 m depth range and corresponding regression lines for stations in the central part of the Labrador Basin for the period 1996–2015

2015 AR7W SF_6 (fmol L-1)

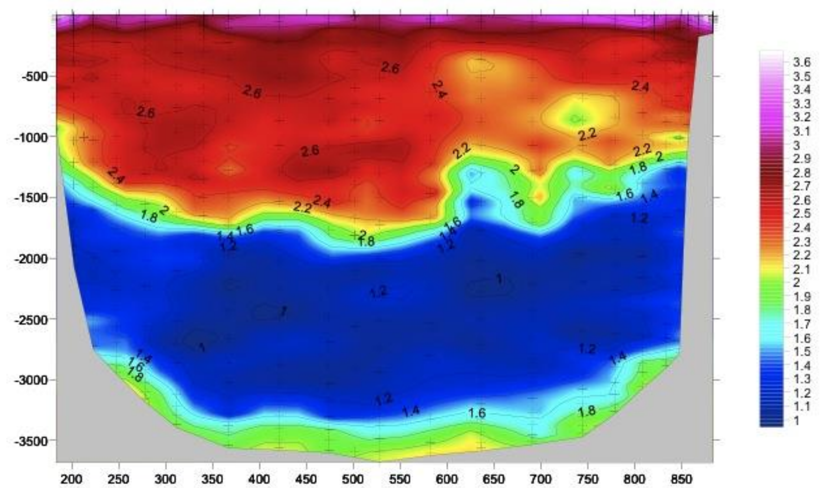

2015 AR7W Line CFC12 (pmol L-1)

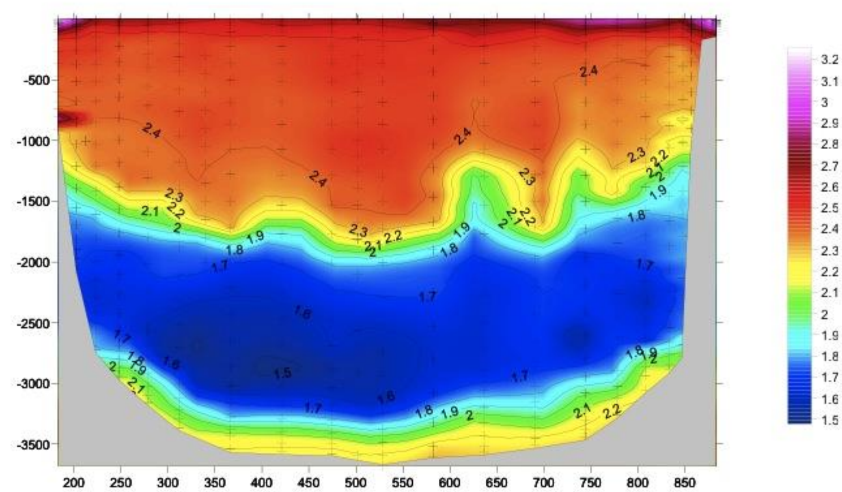

Fig.10. Profiles of transient tracers along the AR7W section. Top: dissolved SF_6 concentration in units of 10^{-15}moles per kilogram seawater. Bottom: CFC-12 concentration in units of 10^{-12} moles per kilogram.

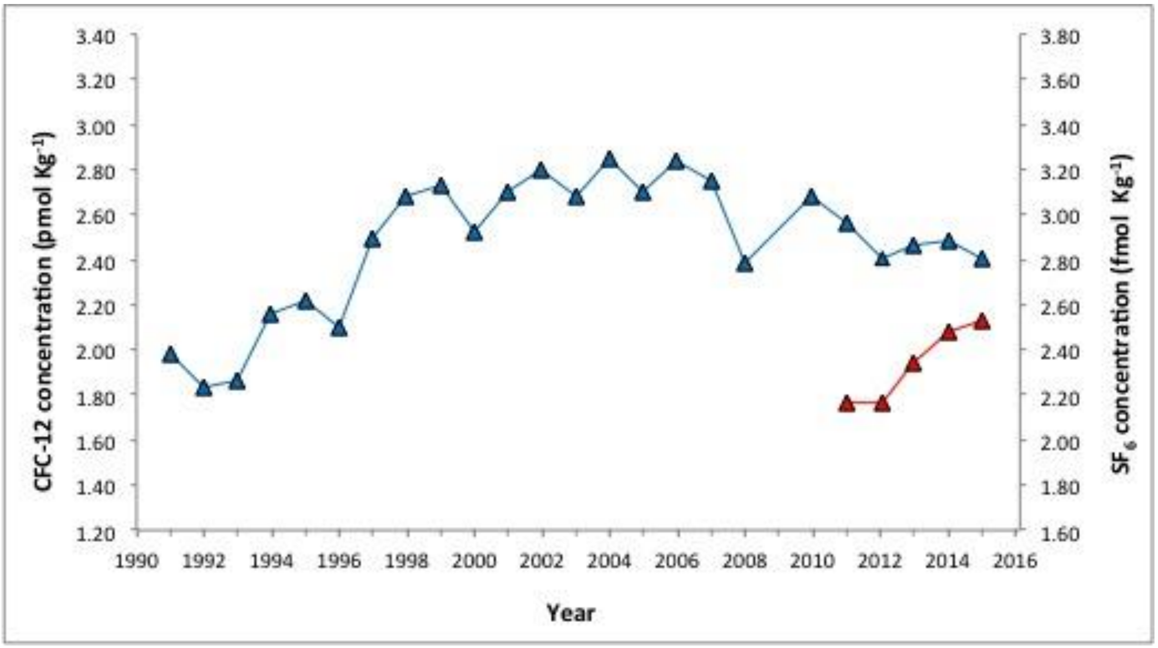

Fig. 11. Annual mean concentrations of CFC-12 (blue) and SF_6 (red) in newly-ventilated Labrador Sea Water (defined as 150<500 m in the central part of the Labrador Sea Basin) from 1991 to present. SF_6 measurements began in 2011.

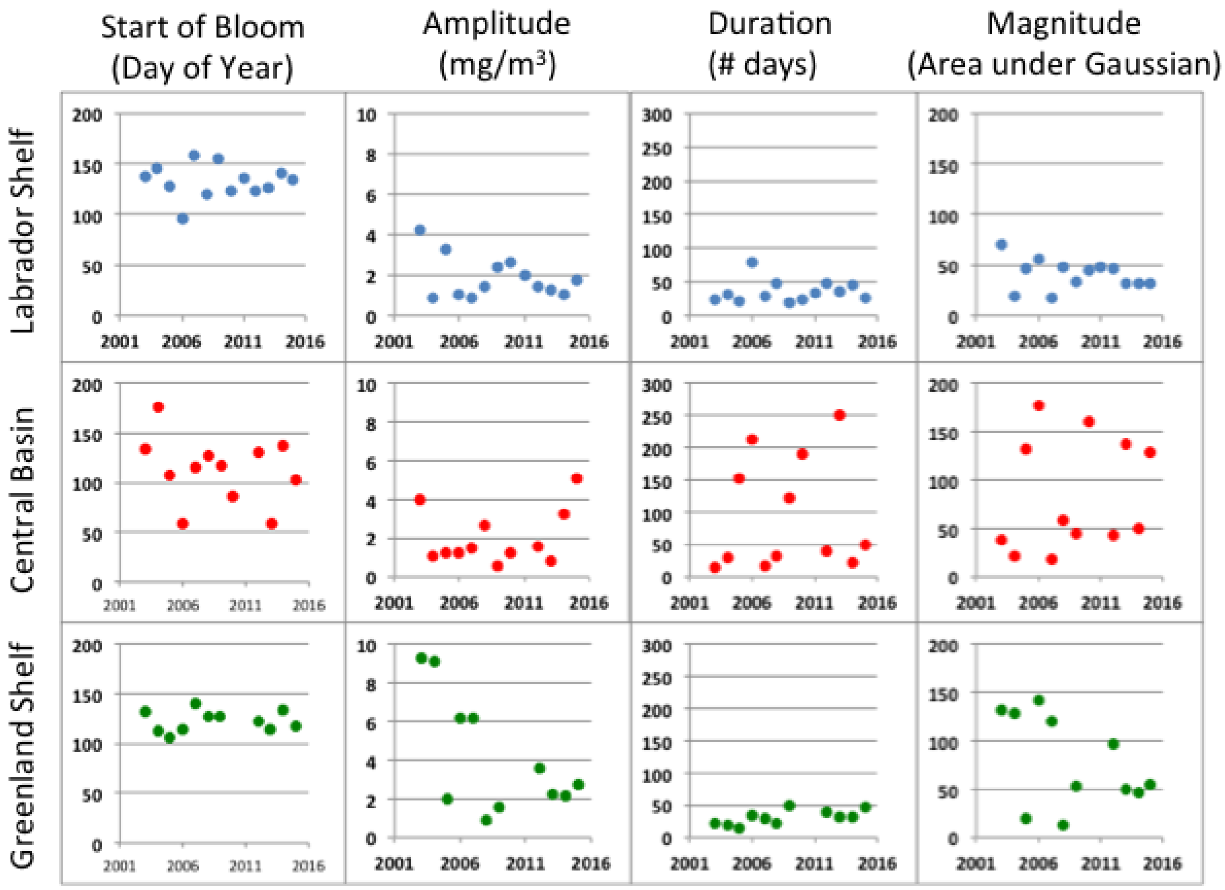

Fig. 12. Phytoplankton bloom characterisation using fitted Gaussian curve to define the start of the bloom, its amplitude (mg/m^3), its duration in number of days and its magnitude corresponding to the area under the curve (Zhai et al.,1991). Central Basin and Greenland Shelf are the combination of multiples large bloom.

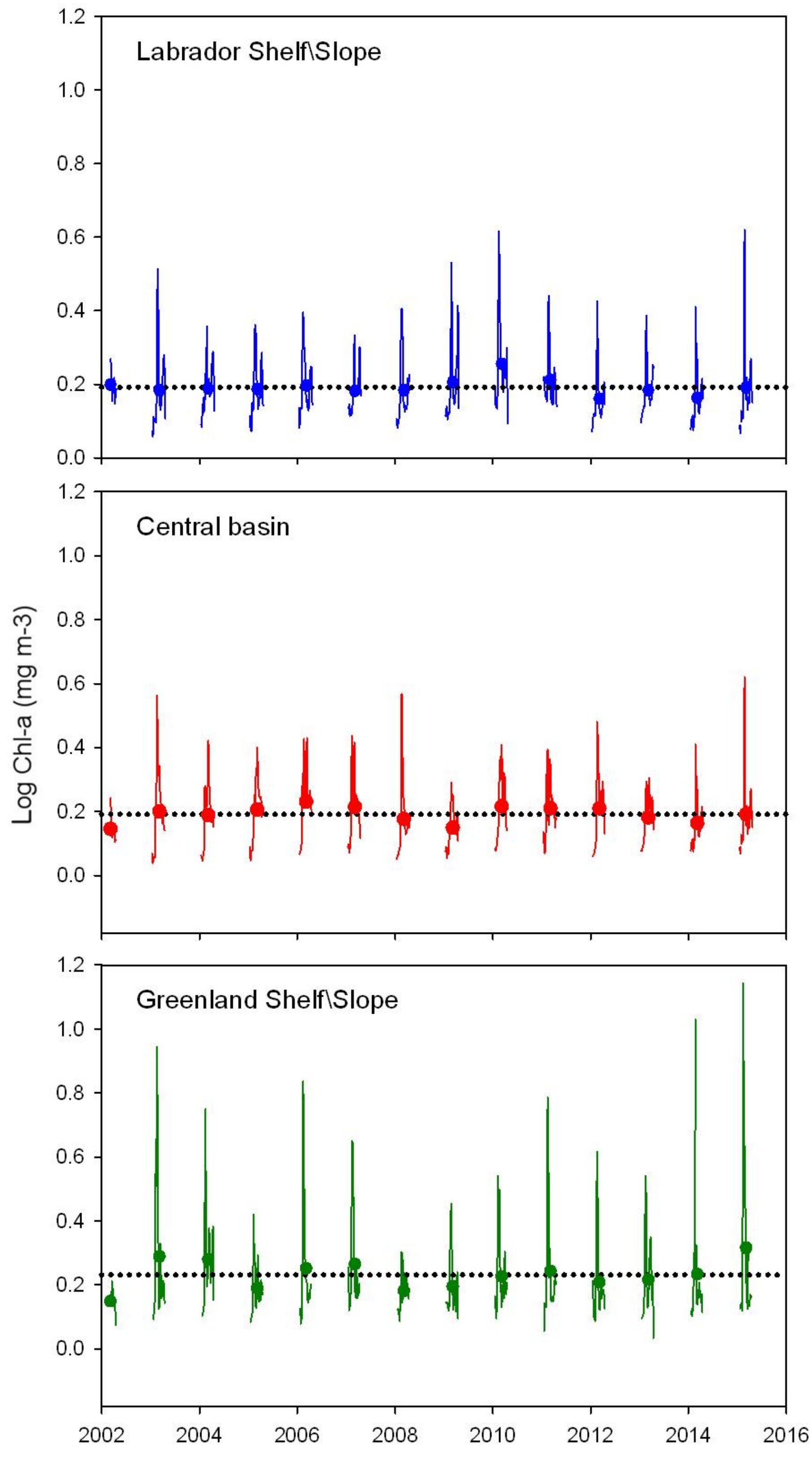

Fig.13. Chlorophyll-*a* normalized anomaly and SST anomaly time series (2003-2015) for Labrador shelf (left column), Labrador Basin (middle column) and Greenland Shelf (right column). Estimated from bi-weekly MODIS data. Lines indicate biweekly anomalies, circles indicate annual average anomalies.

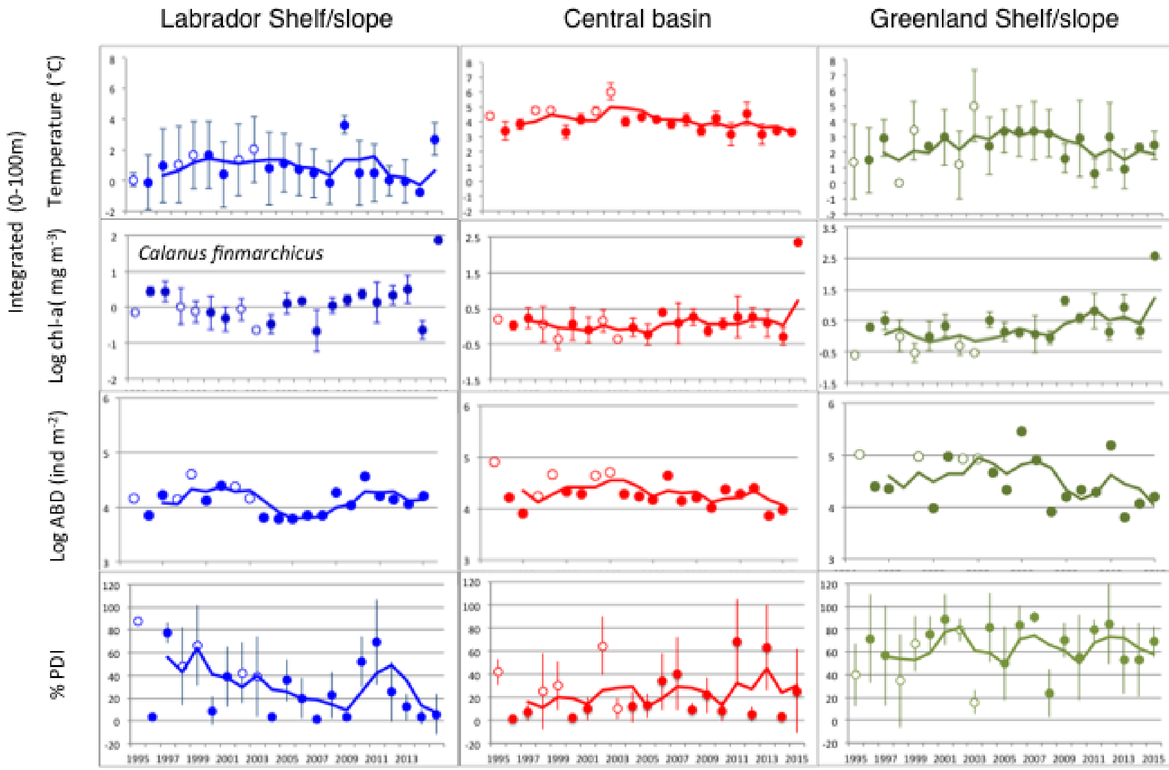

Fig. 14. Upper ocean (z<100m) average SST, chlorophyll-a abundance (Log mg m-*3*), *Calanaus finmarchicus* abundance (Log n ind m^{-2}), and %PDI (from top to bottom panel) on AR7W sampled in spring or early summer from 1994 to 2015. Circles indicate mean value for stations designated within each region, open symbols represents years sampled later in June, error bars indicate among-station standard deviation, and heavy line indicates 3-year running average of the time series.

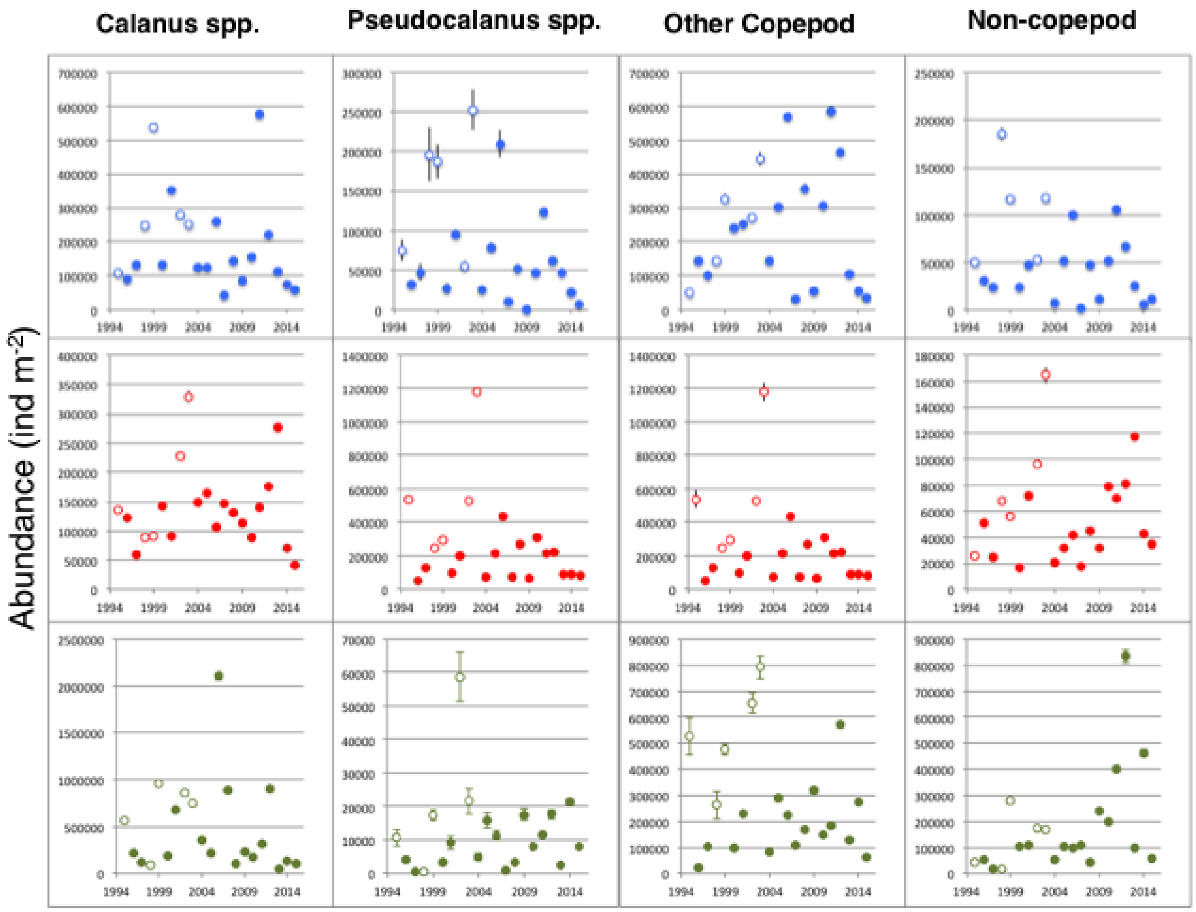

Fig. 15. Time series of the abundance in individuals per m2 for the Calanus spp., Pseudocalanus spp, other copepod species grouped together and the rest of the mesozooplankton regroup in the last column of panel under the label non-copepod. Top row in bleu are for the Labrador Shelf/slope, middle row in red are for the Central basin and the bottom row in green are the Greenland/shelf/slope. Error bars are s.e..

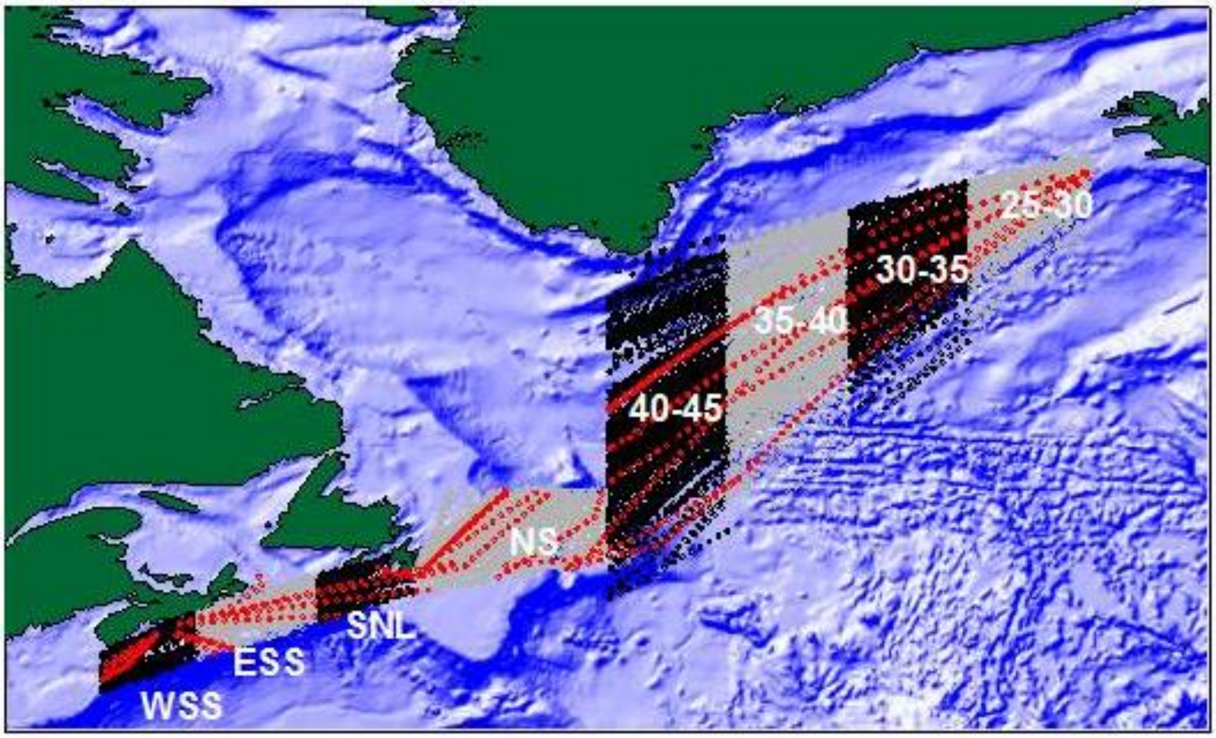

Fig. 16. Continuous Plankton recorder (CPR) lines and stations 1957 to 2013. Stations sampled in 2013 are shown in red. Data are analysed by region. Regions are: Western Scotian Shelf (WSS), Eastern Scotian Shelf (ESS), South Newfoundland Shelf (SNL), Newfoundland Shelf (NS), and between longitudes 40-45^{o}W, 35-40^{o}W, 30-35^{o}W, 25-30^{o}W.

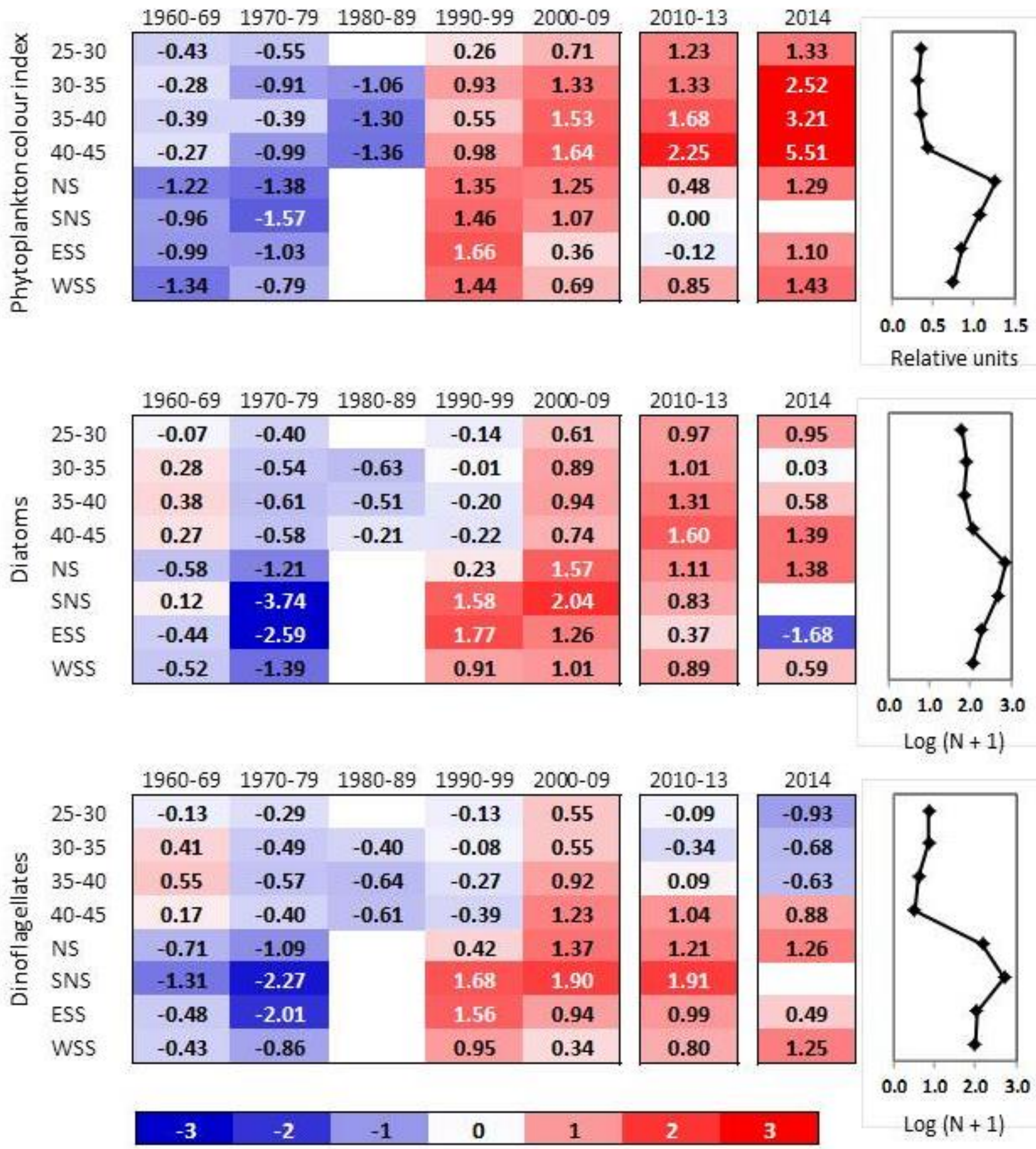

Fig. 17. CPR time series for the annual averages for three indices of phytoplankton concentration, calculated from monthly averages over decadal (1960-2009), tri-annual (2010-2012) or annual (2013) periods for eight regions in the NW Atlantic. Blank cells correspond to years or decades where sampling was too sparse to give annual values. Red (blue) cells indicate higher (lower) than normal values. The climatological averages were calculated from the decadal annual averages between 1960 and 2009, and are shown in the panels on the right. The numbers in the cells are the standardised anomalies. The regions are: Western Scotian Shelf (WSS), Eastern Scotian Shelf (ESS), South Newfoundland Shelf (SNL), Newfoundland Shelf (NS), and between longitudes 40-45°W, 35-40°W, 30-35°W, 25-30°W.

Calanus I-IV	1960-69	1970-79	1980-89	1990-99	2000-09	2010-13	2014
25-30	-0.32	-1.00		0.13	1.20	1.68	0.63
30-35	0.34	-0.92	-0.86	0.06	1.38	2.67	0.83
35-40	0.42	-0.67	-0.69	0.02	0.92	2.90	0.12
40-45	0.02	-0.16	-0.05	-0.01	0.20	1.12	0.22
NS	1.51	0.98		-1.02	-1.47	-0.06	0.83
SNS	0.86	0.77		-1.05	-0.58	0.47	
ESS	0.48	0.35		-0.75	-0.08	-1.56	-0.81
WSS	-0.03	-0.27		-0.14	0.43	-0.29	-0.08

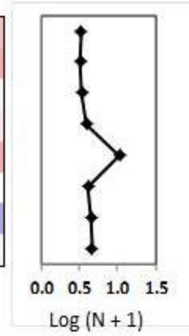

Calanus finmarchicus V-VI	1960-69	1970-79	1980-89	1990-99	2000-09	2010-13	2014
25-30	-0.67	0.17		0.22	0.28	0.72	0.89
30-35	-0.40	0.03	-0.19	0.15	0.41	0.36	0.12
35-40	-0.40	0.21	-0.28	0.29	0.17	0.76	0.17
40-45	-0.41	0.62	-0.36	0.47	-0.32	0.27	-0.17
NS	0.45	0.00		0.17	-0.62	-0.72	2.56
SNS	-0.62	0.71		-0.72	0.64	0.74	
ESS	-0.31	1.24		-1.17	0.25	-1.31	-1.71
WSS	-0.82	1.20		-0.86	0.49	-0.30	-0.78

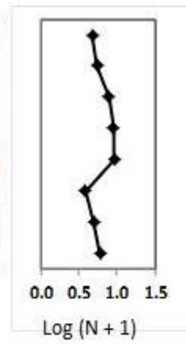

Calanus glacialis	1960-69	1970-79	1980-89	1990-99	2000-09	2010-13	2014
25-30	-0.31	-0.25		-0.21	0.77	-0.06	-0.31
30-35	-0.31	-0.40	-0.38	0.10	0.98	-0.11	-0.40
35-40	-0.34	-0.17	-0.48	-0.05	1.04	0.89	-0.48
40-45	-0.57	-0.11	-0.70	0.41	0.97	0.00	0.08
NS	-0.98	-0.82		1.13	0.66	-0.59	1.79
SNS	-0.65	-0.60		0.19	1.06	0.96	
ESS	-0.45	-0.27		-0.10	0.83	-0.19	-0.91
WSS	-0.22	0.08		-0.49	0.63	-0.06	0.78

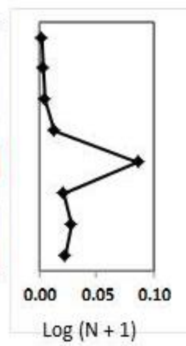

Calanus hyperboreus	1960-69	1970-79	1980-89	1990-99	2000-09	2010-13	2014
25-30	-1.22	2.88		-0.59	-1.07	-1.59	-1.59
30-35	-0.21	-0.17	0.06	0.25	0.06	-0.44	-0.44
35-40	-0.43	-0.28	0.05	0.56	0.09	-0.13	-0.23
40-45	-0.70	-0.30	-0.16	1.12	0.04	0.59	0.43
NS	-0.39	-0.15		0.64	-0.10	-0.52	-0.31
SNS	-0.19	-0.31		-0.25	0.75	-0.27	
ESS	-0.47	-0.50		0.06	0.90	-0.06	-0.60
WSS	-0.39	-0.50		0.36	0.53	0.77	2.81

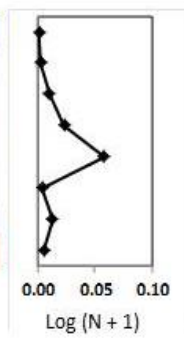

-3	-2	-1	0	1	2	3

Fig. 18. CPR time series for the annual average abundances for four *Calanus* taxa, calculated from monthly averages over decadal (1960-2009), tri-annual (2010-2012) or annual (2013) periods for eight regions in the NW Atlantic. Blank cells correspond to years or decades where sampling was too sparse to give annual values. Red (blue) cells indicate higher (lower) than normal values. The climatological averages were calculated from the decadal annual averages between 1960 and 2009, and are shown in the panels on the right. The numbers in the cells are the standardised anomalies. The regions are: Western Scotian Shelf (WSS), Eastern Scotian Shelf (ESS), South Newfoundland Shelf (SNL), Newfoundland Shelf (NS), and between longitudes 40-45°W, 35-40°W, 30-35°W, 25-30°W.

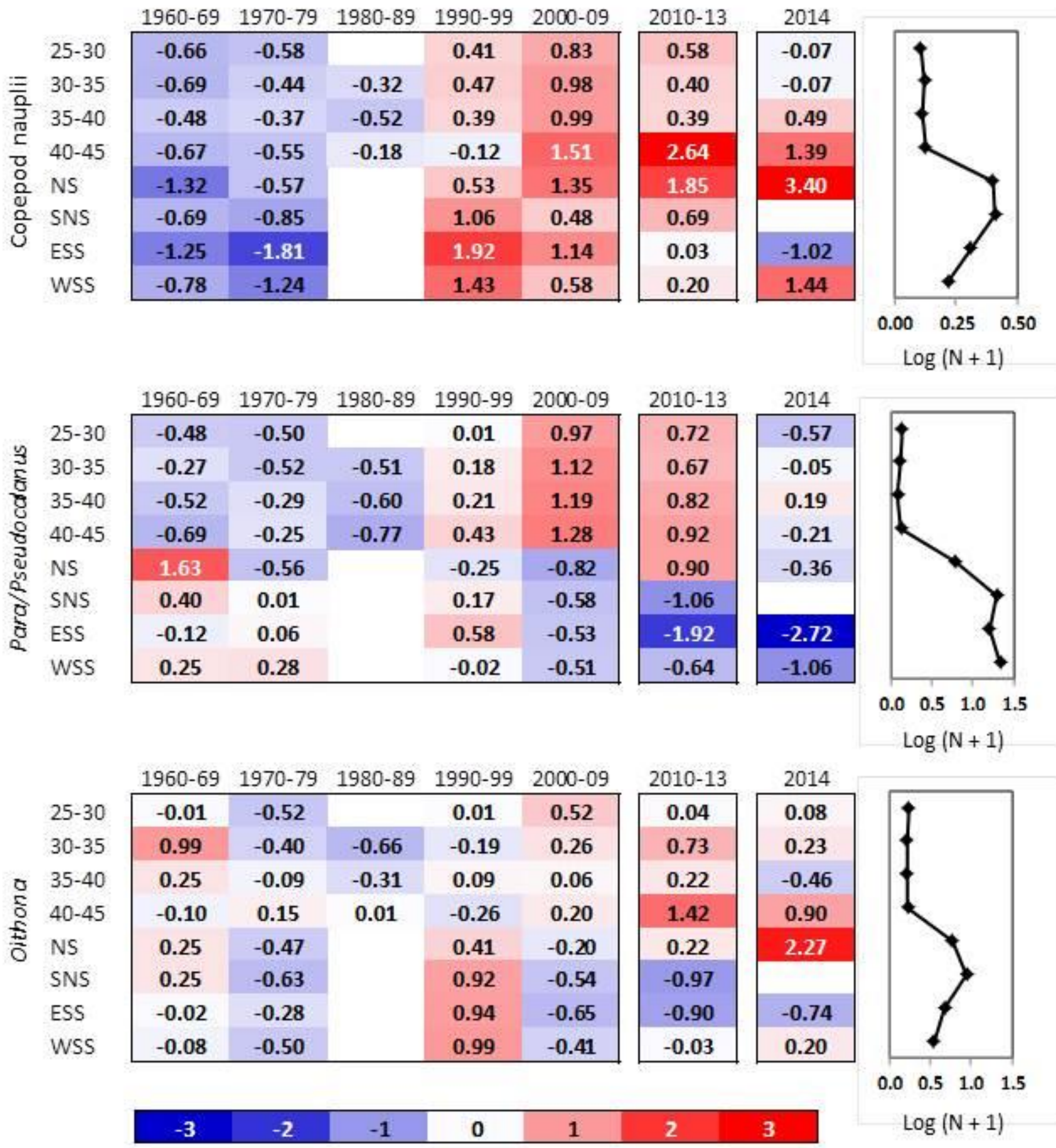

Fig. 19. CPR time series for the annual average abundances for three small copepod taxa, calculated from monthly averages over decadal (1960-2009), tri-annual (2010-2012) or annual (2013) periods for eight regions in the NW Atlantic. Blank cells correspond to years or decades where sampling was too sparse to give annual values. Red (blue) cells indicate higher (lower) than normal values. The climatological averages were calculated from the decadal annual averages between 1960 and 2009, and are shown in the panels on the right. The numbers in the cells are the standardised anomalies. The regions are: Western Scotian Shelf (WSS), Eastern Scotian Shelf (ESS), South Newfoundland Shelf (SNL), Newfoundland Shelf (NS), and between longitudes 40-45°W, 35-40°W, 30-35°W, 25-30°W.

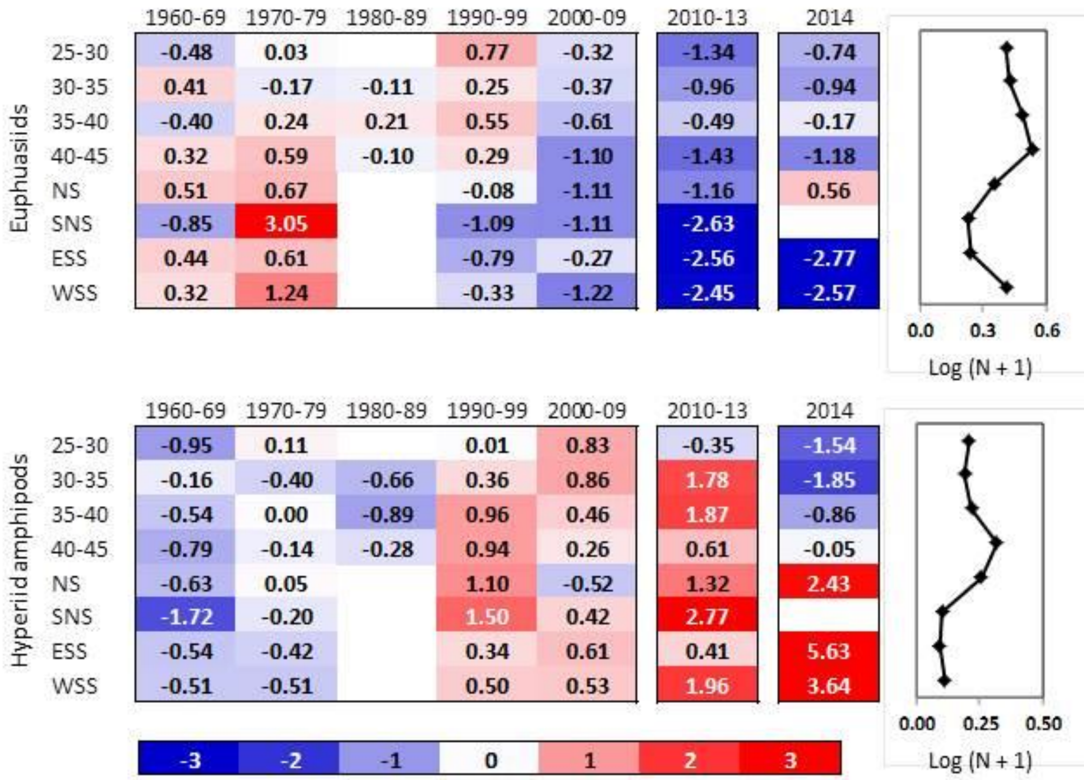

Fig. 20. CPR time series for the annual average abundances for two macrozooplankton taxa, calculated from monthly averages over decadal (1960-2009), tri-annual (2010-2012) or annual (2013) periods for eight regions in the NW Atlantic. Blank cells correspond to years or decades where sampling was too sparse to give annual values. Red (blue) cells indicate higher (lower) than normal values. The climatological averages were calculated from the decadal annual averages between 1960 and 2009, and are shown in the panels on the right. The numbers in the cells are the standardised anomalies. The regions are: Western Scotian Shelf (WSS), Eastern Scotian Shelf (ESS), South Newfoundland Shelf (SNL), Newfoundland Shelf (NS), and between longitudes 40-45°W, 35-40°W, 30-35°W, 25-30°W.

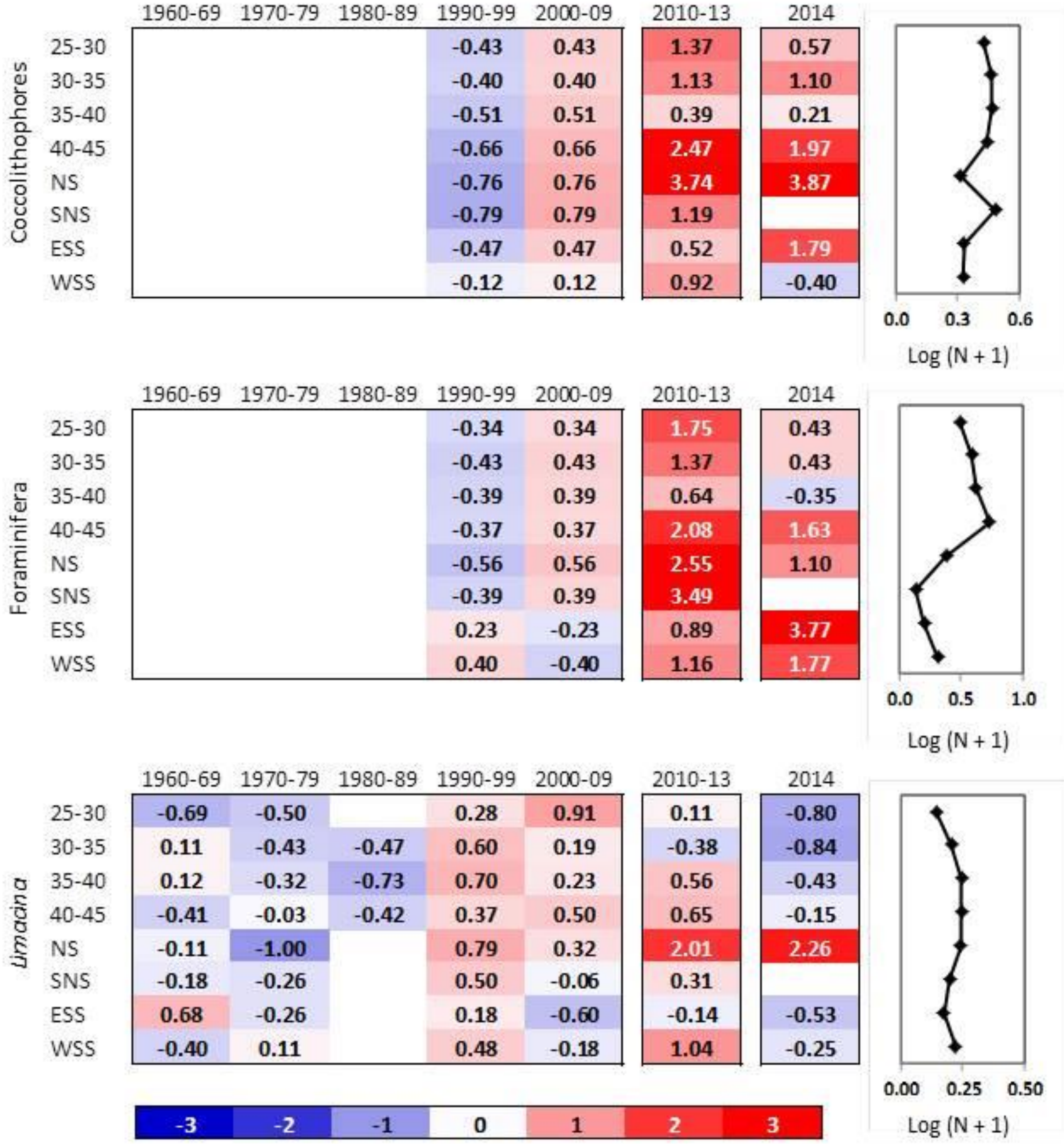

Fig. 21. CPR time series for the annual average abundances for three acid-sensitive taxa, calculated from monthly averages over decadal (1960-2009), tri-annual (2010-2012) or annual (2013) periods for eight regions in the NW Atlantic. Blank cells correspond to years or decades where sampling was too sparse to give annual values. Red (blue) cells indicate higher (lower) than normal values. The climatological averages were calculated from the decadal annual averages between 1990 and 2009 for the coccolithophores and foraminifera, and between 1960 and 2009 for Limacina, and are shown in the panels on the right. The numbers in the cells are the standardised anomalies. The regions are: Western Scotian Shelf (WSS), Eastern Scotian Shelf (ESS), South Newfoundland Shelf (SNL), Newfoundland Shelf (NS), and between longitudes 40-45°W, 35-40°W, 30-35°W, 25-30°W.

Year

	1994	1995	1996	1997	1998	1999	2000	2001	2002	2003	2004	2005	2006	2007	2008	2009	2010	2011	2012	2013	2014	2015
Winter NAO	0.53	1.38	-1.16	-0.42	-0.15	1.29	1.21	-0.73	-0.18	-0.19	-0.81	0.62	-0.19	0.45	0.64	0.29	-2.60	-0.98	1.42	-0.23	1.39	2.08
Air Temperature - Winter	-1.67	-0.96	1.02	-1.02	0.36	1.43	-0.21	1.18	0.27	1.12	3.51	1.60	3.44	3.03	-1.94	2.29	4.61	2.60	0.12	2.41	-0.36	-1.37
- Spring	-0.69	0.78	0.87	1.12	0.65	0.95	-0.06	0.36	0.04	0.01	0.83	2.01	2.10	0.19	1.12	-0.18	2.11	-1.22	1.03	-0.18	-0.28	-0.63
SST - Winter	-0.84	-0.11	0.19	0.23	0.85	0.88	0.12	0.62	0.77	1.15	2.25	1.34	1.10	1.60	-0.30	1.05	1.84	2.43	0.04	1.55	0.15	
- Spring	-0.31	-0.10	0.37	0.75	0.64	0.10	0.06	0.74	-0.19	0.64	0.37	1.00	0.81	0.56	0.20	-0.10	1.49	-0.39	0.29	0.62	-0.29	
Ocean colour (Chlorophyll-*a*)																						
Labrador Shelf/Slope									-0.30	-0.26	-0.51	-0.48	-0.16	-0.78	-0.47	0.44	2.51	0.38	-1.31	-0.67	-1.24	0.04
Central Labrador Sea									-1.67	0.51	-0.15	0.35	1.22	0.74	-0.23	-1.48	0.72	0.47	0.67	-0.54	-1.01	0.16
Greenland Shelf/Slope									-1.30	1.71	0.78	-0.77	0.72	0.61	-0.92	-0.65	-0.17	0.52	-0.29	-0.26	0.58	2.60
SST median anomaly (AVHRR)																						
Labrador Shelf/Slope				-0.02	0.02	-0.40	-0.31	-0.42	-0.57	0.26	0.34	0.26	0.47	-0.37	0.76	-0.28	0.04	0.09	0.47	-0.64	-0.32	-0.34
Central Labrador Sea				1.03	0.07	-0.54	-0.70	-0.14	-0.43	0.42	0.35	0.49	0.63	0.27	0.18	-0.37	0.73	-0.32	0.05	-0.10	0.08	-0.68
Greenland Shelf/Slope				-0.55	-0.81	-1.00	-0.85	-0.38	-0.32	1.02	0.54	0.60	-0.30	-0.28	-0.56	-0.04	1.17	-0.64	0.11	-0.11	-0.01	-0.59
Continuous plankton recorder																						
Phytoplankton Colour Index (Based on the climatological values for 1994-2012)																						
WSS	-0.45	2.03	1.01	-1.31	-0.31	2.03	-0.43	0.69	-0.45	-0.05	-0.65	-0.25	-0.29			-0.73	-0.93	-0.72	-0.15	0.80	1.33	
EES	-0.73	1.51	1.83	0.27	1.51	-0.17	-1.08	-0.38	0.00	0.20	-0.07	-0.53	-1.09				-1.27	-0.71	-1.56	-0.58	2.52	
SNL	-1.38	0.94	0.64	-1.47	1.95	-0.14	-0.68	-0.13		1.09	-0.07	0.2	0.12				-1.16	-0.09	-1.84		3.21	
NLS	-0.58	-0.09	2.55	0.31	0.14	-1.52	0.34	0.4	1.21	-0.03	-0.62	-0.39	-0.86				-0.87	-1.58	-1.34	0.44	5.51	
40_45	1.19	-0.65	-0.19	-1.97	-0.72	1.68	-0.18	-0.01		0.41	-1.52	0.22	0.2			0.96	-0.6		0.45	2.30	1.29	
35_40	0.18	-1.66	0.74		-2.11	0.82	0.05	0.94	0.21	0.12	-1.04	0.44	1.02				0.53		-0.13	1.53		
30_35	0.81	1.58	-0.91		-1.31	0.30	-0.60	0.66	-0.65	0.90	0.47	-0.26	1.04			-1.95	-0.08		-0.76	1.24	1.1	
25_30	-0.67	0.32	-1.83		0.25	1.08	-0.72	-0.17		2.25	-0.65	-0.67	0.41			-0.03	0.43		-0.45	1.49	1.43	

-3	-2	-1	0	1	2	3

Fig. 22. Normalised annual and/or seasonal anomaly of physical and biological variables integrated over large spatial scales estimated using NCEP , remote sensed data or Continuous plankton recorder (CPR) between 1994 and 2015.

Year	1994	1995	1996	1997	1998	1999	2000	2001	2002	2003	2004	2005	2006	2007	2008	2009	2010	2011	2012	2013	2014	2015
Temperature (0-100m)																						
Labrador Shelf/Slope		-0.99	-1.16	-0.04	0.00	0.68	0.70	-0.64	0.35	1.06	-0.22	0.15	-0.32	-0.58	-1.21	2.78	-0.56	-0.52	-1.06	-1.13	-1.89	1.80
Labrador basin		0.23	-1.24	-0.59	0.80	0.83	-1.36	-0.07	0.74	2.72	-0.30	0.18	-0.06	-0.52	-0.13	-1.25	0.01	-1.53	0.49	-1.55	-1.23	-1.32
Greenland Shelf/Slope		-1.32	-1.24	0.18	-2.67	0.66	-0.33	0.24	-1.53	2.24	-0.31	0.63	0.60	0.64	0.48	-1.10	0.16	-2.05	0.28	-1.79	-0.37	-0.27
TIC anomalies			-1.59	-1.86	-1.18	-0.84	-0.45	-0.45	0.26	0.36	0.47	0.74	0.58	0.64	1.29	0.86	1.17	0.10	1.54	2.04	1.96	2.24
pH anomalies			2.07	0.67	0.23	0.88	0.70	1.38	0.12	-0.37	-0.87	-0.69	-0.31	-0.65	-0.86	-0.55	-1.76	-0.34	-1.75	-2.46	-2.28	-1.47
Silicate	2.329	1.252	0.839	0.522	-0.356	0.306	0.582	0.177	0.515	-0.162	-0.771	-1.118	-0.168	-1.4	0.011	-1.133	-1.426	-1.653	-1.292	-0.451	-1.445	
Chlorophyll-a (Log mg m^3)																						
Labrador Shelf/Slope		-0.16	0.44	0.44	0.03	-0.12	-0.16	-0.32	-0.06	-0.64	-0.48	0.12	0.17	-0.66	0.06	0.20	0.38	0.14	0.33	0.51	-0.63	1.88
Labrador bassin	-0.07	0.20	0.01	0.23	0.05	-0.36	0.06	-0.11	0.15	-0.35	-0.03	-0.24	0.40	0.08	0.25	-0.13	0.07	0.26	0.25	0.08	-0.29	2.33
Greenland Shelf/Slope	-0.10	-0.62	0.28	0.50		-0.54		0.34	-0.30	-0.53	0.53	0.13	0.10	0.06	-0.03	1.14	0.58	0.81	0.14	0.94	0.18	2.55

Mezozooplankton (Normalized anomalies)

	1994	1995	1996	1997	1998	1999	2000	2001	2002	2003	2004	2005	2006	2007	2008	2009	2010	2011	2012	2013	2014	2015
Calanus spp																						
Labrador shelf/slope		-0.67	-0.83	-0.48	0.44	2.77	-0.46	1.27	0.70	0.47	-0.53	-0.55	0.56	-1.18	-0.39	-0.84	-0.28	3.08	0.23	-0.63	-0.93	-1.05
Labrador bassin		-0.02	-0.23	-1.19	-0.74	-0.71	0.11	-0.71	1.41	2.96	0.20	0.44	-0.47	0.16	-0.10	-0.37	-0.75	0.06	0.61	2.15	-1.00	-1.46
Greenland shelf/slope		0.07	-0.59	-0.79	-0.84	0.83	-0.66	0.28	0.62	0.41	-0.34	-0.61	3.02	0.68	-0.83	-0.57	-0.69	-0.43	0.73	-0.92	-0.76	-0.8
Pseudocalanus & Scollicithricellla																						
Labrador shelf/slope		-0.15	-0.69	-0.50	1.38	1.27	-0.76	0.10	-0.40	2.09	-0.77	-0.10	1.55	-0.97	-0.44	-1.09	-0.51	0.45	-0.32	-0.51	-0.83	-1.02
Labrador bassin		-0.13	-0.84	-0.15	-1.18	-0.77	-0.68	0.08	0.15	-1.52	-0.71	0.09	-0.21	-0.75	2.15	2.05	0.91	1.68	1.25	0.41	1.22	3.13
Greenland shelf/slope		-0.08	-0.54	-0.78	-0.79	0.39	-0.58	-0.19	3.31	0.69	-0.48	0.29	-0.04	-0.75	-0.60	0.41	-0.26	-0.01	0.41	-0.66	0.68	-0.27
Other Copepoda																						
Labrador shelf/slope		-1.22	-0.60	-0.87	-0.60	0.61	0.04	0.13	0.25	1.41	-0.59	0.46	2.22	-1.34	0.82	-1.19	0.47	2.32	1.53	-0.84	-1.18	-1.33
Labrador bassin		0.85	-0.86	-0.58	-0.16	-0.01	-0.69	-0.34	0.83	3.11	-0.78	-0.27	0.50	-0.77	-0.07	-0.81	0.06	-0.27	-0.25	-0.72	-0.71	-0.75
Greenland shelf/slope		1.10	-1.17	-0.81	-0.08	0.88	-0.84	-0.23	1.68	2.30	-0.90	0.04	-0.27	-0.78	-0.50	0.17	-0.59	-0.45	1.31	-0.68	-0.03	-0.99
Others																						
Labrador shelf/slope		-0.15	-0.55	-0.69	2.60	1.21	-0.68	-0.21	-0.08	1.22	-1.02	-0.13	0.85	-1.12	-0.20	-0.93	-0.12	0.96	0.19	-0.66	-1.04	-0.94
Labrador bassin		-0.70	-0.05	-0.73	0.41	0.08	-0.93	0.50	1.15	2.93	-0.84	-0.55	-0.29	-0.91	-0.21	-0.55	0.70	0.47	0.74	1.71	-0.25	-0.47
Greenland shelf/slope		-0.89	-0.76	-1.22	-1.22	2.08	-0.13	-0.03	0.77	0.72	-0.74	-0.10	-0.21	-0.07	-0.90	1.61	1.09	3.62	9.05	-0.17	4.39	-0.68

-3	-2	-1	0	1	2	3

Fig. 23. Normalised anomaly of physical, chemical and biological in-situ measurements on the AR7W line between 1994 and 2015.